

We thank referee #1 R Subramanian for the many constructive comments and suggestions which helped to improve the manuscript. In order to improve readability, we numbered each reviewer comment and its corresponding response in the style R1-C1 for reviewer 1 comment 1 and R1-A1 for reviewer 1 answer to comment 1, respectively. Comments by the reviewer are given in black, our response to the comments are shown in red, and modified text in the revised manuscript are given in green. Supporting information (SI) has been added. In the following, we provide a point-by-point response to all comments.

RC1: 'Important submission on an understudied region', R Subramanian, 05 Jul 2021

R1-C1: Deabji et al. present initial (five-month) PM₁₀ and chemical composition results from a new monitoring station at a remote elevated site in Northern Africa. Given the lack of data from this region, this is an important contribution that will lead to greater understanding of aerosol sources in Northern Africa. Unfortunately, the manuscript as presented is hard to read and could benefit from restructuring/reorganization. Some of the conditions and comparisons seem arbitrary.

R1-A1: The manuscript has been copy-edited and large parts of the manuscript have been re-written and thoroughly improved. Figures have been improved. Grammatical errors have been corrected and the language has been edited to be more concise throughout. The references have been edited to avoid errors in the citations. The structure of the manuscript has been improved. The classification criteria have been reconsidered, therefore some of the results have been modified. Some sections have been combined to improve readability, comparisons, and avoid repetition. A point-by-point description of the changes made to the manuscript is given in the following.

R1-C2: For example, they report PM₁₀ concentrations during "background" periods were up to 20 µg/m³ - but that is because the authors set 20 µg/m³ as the upper limit defining "background" periods.

R1-A2: The choice of the background definition was motivated by different studies such as Puxbaum et al., 2004; Vardoulakis and Kassomenos, 2008; Karaca et al., 2009; Harrison et al., 2004; Escudero et al., 2006 who suggested that the reference could be at 20 µg m⁻³. However, as recommended by the reviewer the lowest fifth (5th) percentile of PM₁₀ mass concentrations has now been considered as the baseline threshold. This can be easily seen in the new PM₁₀ variation Figure (Fig. 3A). Based on these new criteria, the PM₁₀ < 12 µg m⁻³ was considered as background. The number of samples that met this condition was 10 and the mean concentration was about 10.9 µg m⁻³. The frequency and the probability density function of mass concentrations and wind speed were calculated for background samples (Fig. S3). The thresholds chosen are in line with the results obtained from statistical calculations, as highlighted with the blue bars in the frequency and probability density function Figures below.

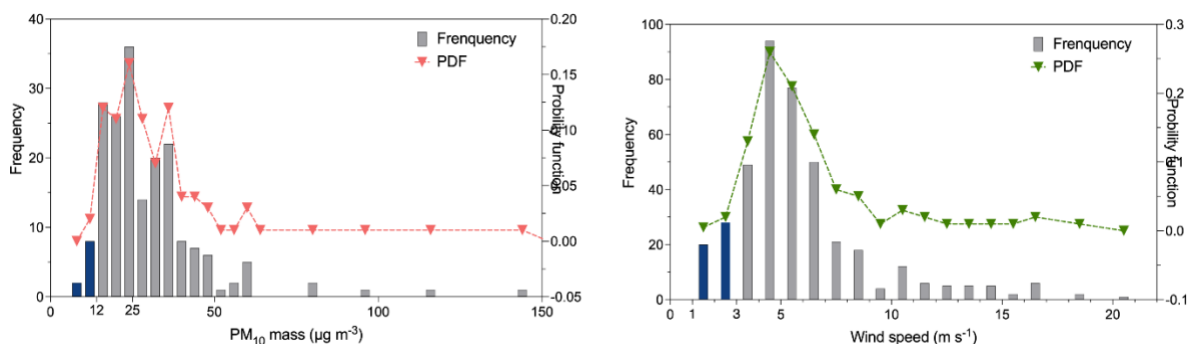


Figure S3. Frequency distribution and corresponding probability density function of PM₁₀ mass and wind speed during the sampling period.

The following text has been added on the manuscript on lines 318-323:

“To establish a reference baseline and evaluate the background conditions at the site, the lower 5th percentile of the PM₁₀ concentrations ($PM_{10} < 12 \mu\text{g m}^{-3}$) was found to be representative of remote background aerosol conditions. The PM₁₀ frequency and probability density function as shown in Fig. S3 confirmed this observation. The samples within this PM concentration range had similar air mass trajectories and typical meteorological conditions with low wind speeds $< 3 \text{ m s}^{-1}$. The air masses typically traveled in the free troposphere at about 1000 m above sea level, crossing the North-Atlantic Ocean before arriving at the site within the past 96 h.”

R1-C3: They also excluded local pollution from "background" and then present results saying these were dominated by local dust – this again is a result of excluding other local sources.

R1-A3: The former criterion has been revised and new chemical composition of these samples evaluated. The current criteria also consider both local and regional sources during background conditions especially from anthropogenic activities such as local road dust resuspension from cars accessing the site. A corresponding sentence has been added to the manuscript in line 324 and now reads:

“These conditions were, however, not free from local and regional pollution from point sources such as dust resuspension from the cars accessing the site.”

R1-C4: A better approach might be to pick the lowest fifth (5th) or tenth (10th) percentile of PM₁₀ mass concentrations and describe that as background condition.

R1-A4: We thank the reviewer for the suggestion which is crucial for the selection of background samples. As recommended by the reviewer the lowest fifth (5th) percentile of PM₁₀ mass concentrations has now been considered as the baseline threshold for the background conditions. This can be easily seen in the new PM₁₀ variation figure, as shown below in the updated Fig. 3a. Based on these new criteria, the maximum PM₁₀ during these conditions was 12 $\mu\text{g m}^{-3}$. The number of samples that met this condition was 10 and the mean concentration was about 10.9 $\mu\text{g m}^{-3}$. A corresponding line has been added on the manuscript on lines 326-329:

“Consequently, the average background PM₁₀ mass concentration at the Middle-Atlas was 10.9 $\mu\text{g m}^{-3}$, which was found to be stable and representative of periods of little external influence. In comparison, Benchrif et al. (2018) reported background PM₁₀ values for Northern Morocco with an average of 12.2 $\mu\text{g m}^{-3}$, which is very similar to the concentrations determined in this study, 10.9 $\mu\text{g m}^{-3}$.”

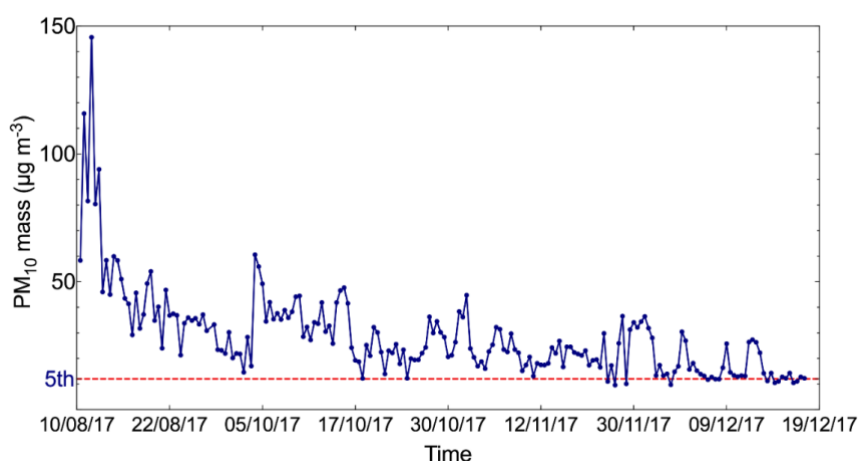


Figure 3. (A) Time series of daily PM₁₀ mass

R1-C5: Similarly, the comparisons with Delhi and Kathmandu seem out of place, as pollution in urban centers especially these locations is very complex and unlike AM5. Since the focus of this manuscript is on AM5, even comparing Moroccan cities (from other published literature, not this work) to Delhi is out of place in this manuscript.

R1-A5: The comparison section has been restructured and rewritten and Table 3 has been modified. The choice of stations was redesigned with a focus on remote background stations. The GAW network database was used as a reference for site selection. Sites like Jungfrauoch, Mt. Everest, Mt. Cimone, and Puy de Dôme were introduced to optimize and make the comparison more relevant. The choice of urban stations was also questioned, therefore only urban stations located in Morocco are now included. The update of Table 3 is as follows:

Table 3. Average mass concentration of PM₁₀ from other high-altitude sites and urban sites in Morocco reported in the literature and ordered according to their altitudes.

N°	Site	Site type	Sampling Period	Altitude (m)	PM ₁₀ (µg m ⁻³)	References
1	Mt. Everest, Nepal	High altitude	Feb 2006-May 2008	5079	6	Decesari et al., 2010
2	Lhasa, Tibet	High altitude	Jan-Feb 2006	3663	37	Wang et al., 2015
3	Jungfrauoch, Switzerland	High altitude	Feb-Mar 2005	3580	3	Cozic et al. 2008
4	Izaña, Canary Islands	High altitude	Feb 2008-Aug 2013	2400	46	García et al., 2017
5	Mount Cimone, Italy	High altitude	Jun-Aug 2004	2165	16	Marenco et al. 2006
6	Atlas (AM5), Morocco	High altitude	Aug-Dec 2017	2100	29	Present study
7	Puy de Dome, France	High altitude	Apr 2006-Apr 2007	1465	6	Bourcier et al. 2012
8	Mahabaleswar, India	High altitude	Jun 2012-May 2013	1348	37	Leena et al., 2017
9	Djarjeeling, India	High altitude	Jan-Dec 2005	2194	29	Chatterjee et al. 2010
10	Marrakech, Morocco	Urban	2009-2012	465	55	Inchaouh et al., 2017
11	Meknes, Morocco	Urban	Mar 2007-Apr 2008	546	75	Tahri et al., 2012
12	Tetouan, Morocco	Urban	May 2011-Apr 2012	105	31	Benchrif et al., 2018
13	Kenitra, Morocco	Urban	Feb 2007-Feb 2008	26	110	Tahri et al., 2017

In addition, Table 4 in the previous version, which presented the chemical composition only during background conditions has been modified and now labeled Table 5. The new Table 5, presents the chemical composition for the entire sampling period comparing the values with those of other high-altitude sites, as shown below.

Table 5. Concentrations of main aerosol chemical species in PM₁₀ (ng m⁻³) at AM5 compared to other high altitude mountain stations. Data are reported in the format average (mean ± standard deviation) and NA: not available. Notice that the concentrations of PM₁₀ mass are given in µg m⁻³. ^a Present study; ^b Bourcier et al. 2012; ^c Chatterjee et al. 2010; ^d Marenco et al. 2008; ^e Decesari et al., 2010.

Elements	Mt. Atlas, Morocco ^a	Mt. Puy de Dome, France ^b	Mt. Himalaya, India ^c	Mt. Cimone, Italy ^d	Mt. Everest, Nepal ^e
Altitude (m a.s.l.)	2100 m	1465 m	2194 m	2165 m	5079 m
Samples	190	NA	111	57	99
Period	Aug-Dec 2017	Apr 2006-Apr 2007	Jan-Dec 2005	Jun-Aug 2004	Apr 2006 - May 2008
Mass load	29.1 ± 17.3	5.6 ± 4.6	29.5 ± 20.8	16.1 ± 9.8	5.6 ± 4.6
OC	1069 ± 818	NA	NA	NA	800 ± 637
EC	247 ± 134	NA	NA	NA	115 ± 132
Na ⁺	186 ± 231	NA	2200 ± 2000	NA	24.2 ± 22.5
K ⁺	42 ± 35	NA	310 ± 210	NA	34 ± 32
Ca ²⁺	649 ± 579	15.5 ± 10.2	130 ± 10	360 ± 550	138 ± 90
Mg ²⁺	60 ± 50	NA	120 ± 60	NA	19.3 ± 7.2
Cl ⁻	80 ± 133	NA	2350 ± 1500	82 ± 98	22 ± 46
NH ₄ ⁺	298 ± 220	297 ± 276	50 ± 40	1400 ± 800	175 ± 183
NO ₃ ⁻	859 ± 687	510 ± 980	950 ± 200	840 ± 770	170 ± 223
SO ₄ ²⁻	941 ± 848	1380 ± 1160	3500 ± 2100	3500 ± 2000	394 ± 329
Al	443 ± 830	NA	NA	300 ± 460	740
Fe	486 ± 728	NA	NA	260 ± 440	NA
Ti	37 ± 45	NA	NA	30 ± 50	NA
V	3.5 ± 12.2	NA	NA	3.1 ± 1.5	NA
K	174 ± 156	NA	NA	160 ± 210	NA
Cr	4.3 ± 5.2	NA	NA	NA	NA
Ni	2.4 ± 3.1	NA	NA	1.4 ± 0.5	NA
Cu	1.2 ± 3.1	NA	NA	2.9 ± 3.1	NA
Zn	8.6 ± 6.2	NA	NA	9.9 ± 6.6	NA
Pb	4.8 ± 4.5	NA	NA	3.9 ± 2.4	NA
Mn	12.4 ± 39.3	NA	NA	6.2 ± 7.0	NA

The comparison of the chemical composition at AM5 has been added with other high altitude sites in section 3.3. The corresponding sentences have been added as follows:

In lines 395-398: “For instance, the high-altitude site in Mt. Cimone, Italy recorded several days with African dust transport which influenced the chemical composition (Marenco et al., 2006). However, the Saharan dust concentration at AM5 (17.7 µg m⁻³) is approximately 4 times higher than at Mt. Cimone (4 µg m⁻³).”

In lines 398-400: “Nevertheless, the average concentrations of elements such as Al, Fe, Ti, and Mn, are comparable with the values reported in Mt. Cimone, Italy (Marenco et al., 2006), Table 5. However, the calcium, concentration at the AM5 (0.65 ± 0.58 µg m⁻³), was 2 times higher than the concentration recorded in Mt. Cimone.”

In lines 401-402: “Furthermore, the calcium concentration was 5 times higher than the concentration recorded at other high-altitude station such as Mt. Himalaya and Mt. Everest (Chatterjee et al. 2010; d; Decesari et al., 2010).”

In lines 404-405: “Some studies have reported the high content of calcite in the soils of Northern Morocco $1.07 \mu\text{g m}^{-3}$ which confirms the predominance of calcium-rich in the Atlas regions (Desboeufs and Cautenet, 2005; Kandler et al., 2009; Benchrif et al., 2018).”

In lines 432-435: “The study of Decesari et al. 2010 reported similar concentrations of OC ($0.8 \pm 0. \mu\text{g m}^{-3}$), and lower EC ($0.11 \pm 0.13 \mu\text{g m}^{-3}$) concentrations in PM10 at the Himalayan high-altitude station in Nepal. Furthermore, Sharma et al., 2020 reported higher OC ($5.4 \pm 2.0 \mu\text{g m}^{-3}$) and EC ($2.2 \pm 2.0 \mu\text{g m}^{-3}$) at the high-altitude site of Darjeeling, India most likely due to the higher influence of anthropogenic activities at the site.”

In lines 346-449: “The OC/EC ratio observed at AM5 for BAM was similar to those found in local samples in Northern Morocco with an average of 1.9 (Benchrif et al. 2018). Moreover, the OC/EC ratio shows a slight difference with those observed in Mt. Everest (Decesari et al., 2010) whose ratios varied from 5 to 9.”

In lines 476-481: “The comparison of sodium and chloride concentrations with other high-altitude studies is shown in table 5. The concentrations of Na^+ ($1.8 \pm 2.31 \mu\text{g m}^{-3}$) and Cl^- ($0.80 \pm 1.33 \mu\text{g m}^{-3}$) are several times lower than those at Darjeeling in India which has a concentration of Na^+ and Cl^- , of $2.2 \pm 2.0 \mu\text{g m}^{-3}$ and $2.3 \pm 1.5 \mu\text{g m}^{-3}$, respectively. On the other hand, the concentration of Na^+ and Cl^- were 4 to 8 times higher than the values reported at Mt. Everest station located at an altitude of 5079 m asl. In addition, the concentration of chloride was in good agreement with those observed in Mt. Cimone, Italy, $0.82 \pm 0.98 \mu\text{g m}^{-3}$ ”.

In lines 481-484: “Sea salt concentration observed at the AM5 ($0.45 \mu\text{g m}^{-3}$) was 5 times lower than at Tetouan ($2.46 \mu\text{g m}^{-3}$), a coastal Mediterranean city in northern Morocco, and approximately 20 times lower than Cap Verde Atmospheric Observatory (CVAO) located in the tropical Atlantic Ocean (Benchrif et al. 2018; Fomba et al. 2014).”

In lines 504-508: “Secondary inorganic aerosol over the Atlas Mountains has been compared with the data reported in other high-altitude stations (Table 5). The average concentration of nitrate ($0.8 \pm 0.6 \mu\text{g m}^{-3}$) at AM5 was comparable with those reported in Mt. Himalaya and Mt. Cimone, $0.9 \pm 0.2 \mu\text{g m}^{-3}$ and $0.8 \pm 0.7 \mu\text{g m}^{-3}$, respectively (Chatterjee et al. 2010; (Marenco et al., 2006). However, the concentration of NO_3^- were found to be approximately 2 times higher than the value reported in Puy de Dôme (Bourcier et al., 2012), as shown in Table 5”.

In lines 513-516: “Similar concentrations of ammonium at AM5 ($0.3 \pm 0.2 \mu\text{g m}^{-3}$) were found at Puy de Dôme, France ($0.3 \pm 0.2 \mu\text{g m}^{-3}$), whereas the concentration was 5 times lower than those reported in other high-altitude sites such as the Mt. Himalaya (Chatterjee et al., 2010). This indicates that the influence of ammonium remains relatively low despite the proximity of the site to agricultural activities located in the surroundings of Meknes.”

In lines 517-519: “The concentrations of sulfate ($0.9 \pm 0.8 \mu\text{g m}^{-3}$) over AM5 were comparable with those at Puy de Dôme ($1.3 \pm 1.1 \mu\text{g m}^{-3}$), but were almost 4-5 times lower than all the other hilly stations except Mt. Everest (Decesari et al., 2010).”

R1-C6: I also had a hard time following the paper, and it could benefit from a more organized structure. For example, in the site intercomparison above, the authors compare AM5 with Izana (Moroccan coastal site), then with India/Tibet/Kathmandu, then back to Cape Verde (off the coast of North Africa), then to an unnamed background site in the Mediterranean. This discussion would be more cohesive if AM5 is compared first with all remote sites, then (if at all) with urban sites rather than switching back and forth.

R1-A6: The intercomparison section was rewritten and reworded following the reviewer's recommendations. Starting first with a comparison of station AM5 with remote high-altitude sites, then a comparison with Moroccan urban sites was introduced in the following paragraph. The intercomparison section has been added to the revised manuscript on lines 331-340 and now reads:

“The mean concentration recorded at AM5 from this study ($29.2 \pm 17.3 \mu\text{g m}^{-3}$) agreed well with the PM_{10} concentration of other remote high-altitude sites, such as Darjeeling in Northeastern Himalayas ($29 \mu\text{g m}^{-3}$; Chatterjee et al. 2010), Lhasa in Tibet ($37 \mu\text{g m}^{-3}$; Wang et al., 2015), and Mahabaleshwar in India ($37 \mu\text{g m}^{-3}$; Leena et al., 2017) as presented in Table 3. Other high-altitude stations, such as Izaña, in Canary Islands ($46 \mu\text{g m}^{-3}$) showed much higher PM_{10} , most likely due to the exposure to strong Saharan dust events (García et al., 2017). In contrast, the PM_{10} concentrations at AM5 were considerably higher than the PM_{10} levels recorded in European and Asian high-altitude sites. For example, the average PM_{10} mean value recorded in this study was about twice that of Mount Cimone, Italy ($16 \mu\text{g m}^{-3}$; Marenco et al., 2006) and factor 6 greater than the PM_{10} in Everest Mountain (Decesari et al., 2010) and in Puy de Dôme, France ($6 \mu\text{g m}^{-3}$; Bourcier et al. 2012), and was approximately 10 times greater than the average level in Jungfrauoch ($3 \mu\text{g m}^{-3}$; Cozic et al., 2008).”

R1-C7: when discussing daily and monthly variations, they first discuss August/summer. In the next paragraph, they discuss Oct-Nov-Dec, but midway again discuss August and Saharan influence, then again present winter (Nov-Dec?) results.

R1-A7: The daily and monthly discussion has been restructured in a uniform and consistent paragraph. The variation during summer has been moved to the previous paragraph followed by the discussion on the autumn and winter. The corresponding sentences on lines 234-335 and now read:

“During August, high PM_{10} concentration were mostly related to high wind speeds from southeast wind direction. For example, PM_{10} mass concentration often exceeded $50 \mu\text{g m}^{-3}$ and sometimes even reached up to $145 \mu\text{g m}^{-3}$ during August, when the wind speed was stronger than 9 m s^{-1} .”

R1-C8: Even the winter discussion is inconsistent, as they first say a change in wind direction leads to lower PM₁₀ (which seems unlikely since the populated centers are to the west and wind speeds are high), but then attribute the lower PM to increased precipitation (which is more logical).

R1-A8: We thank the reviewer for this insightful comment. The winter discussion has been modified and the precipitation argument reworded to make it more consistent and uniform. The drop in PM is certainly due to precipitation. The corresponding sentences in lines 347-352 now read:

“A sharp fall in PM concentrations was noticed in November ($22.8 \pm 7.9 \mu\text{g m}^{-3}$) and December ($15.9 \pm 5.6 \mu\text{g m}^{-3}$). Overall, PM₁₀ concentration decreased from the summer to winter by 32%. This trend is most likely due to the increased amount of precipitation (peaks of 852mm) during fall and winter, which can lead to the wash-out effect of aerosol and its components (Holst et al. 2008).”

R1-C9: Skimming the rest of the paper showed continued repetition and disorganized presentation of results - for example, line 822 has the "first insight into aerosol chemical composition..." midway through a paragraph, and then next paragraph also starts with "first high altitude aerosol characterization study..."

R1-A9: The repetitions have been eliminated and the manuscript has been edited. All the copy editing modifications are listed at the end of the response.

R1-C10: I also don't know why sulfate concentration of $1.4 \mu\text{g}/\text{m}^3$ is presented as high when average concentrations at AM5 are $\sim 30 \mu\text{g}/\text{m}^3$ - is that because that sulfate level is high relative to average sulfate at the site? It might help to separate these two results, then.

R1-A10: That sentence was meant to compare the sulfate concentrations with those during background conditions, Therefore, the two results were separated as suggested. In the first instance, the sulfate concentration of MCE is high ($1.2 \pm 0.9 \mu\text{g m}^{-3}$) compared to the average sulfate concentration during background conditions $0.2 \pm 0.2 \mu\text{g m}^{-3}$ at the AM5 site. The corresponding sentences have been added as follows and now read:

In lines 500-501: “In average, the sulfate concentration for MCE ($1.2 \pm 0.9 \mu\text{g m}^{-3}$) was about 5 times higher than background sulfate concentrations ($0.2 \pm 0.2 \mu\text{g m}^{-3}$).”

In lines 517-519: “The concentrations of sulfate ($0.9 \pm 0.8 \mu\text{g m}^{-3}$) over AM5 were comparable with those at Puy de Dôme ($1.3 \pm 1.1 \mu\text{g m}^{-3}$), but were almost 4-5 times lower than all the other hilly stations except Mt. Everest (Decesari et al., 2010).”

R1-C11: The next few sections were lengthy, somewhat repetitive descriptions of chemical composition results. The manuscript may be more readable if the monthly variation and chemical composition results are replaced and reorganized by air mass as winds from different directions seem to hit the site each month.

R1-A11: The manuscript has been restructured by introducing air mass classification before the description of the chemical composition. As a result, the new structure allows the discussion of the results of the chemical composition of the complete period using the interpretation of the influence of the air masses introduced previously, to avoid any repetitions. The modified structure now reads as follow:

3.1 Variation of PM₁₀ mass

3.2 Air mass origins

3.3 Characterization of aerosol chemical composition for the complete measurement period

3.4 Inter-relationship between aerosol components

3.5 Day and night-time variation

3.6 Differences in chemical composition between dust and non-dust events

The section of PM₁₀ mass variation according to month and chemical composition has been reorganized by introducing the influence of air masses and winds coming from different directions. Figure 3 was modified to discuss the variation of PM₁₀ concentration according to the change of wind speed and direction of each month. A new Fig. 3 is shown below.

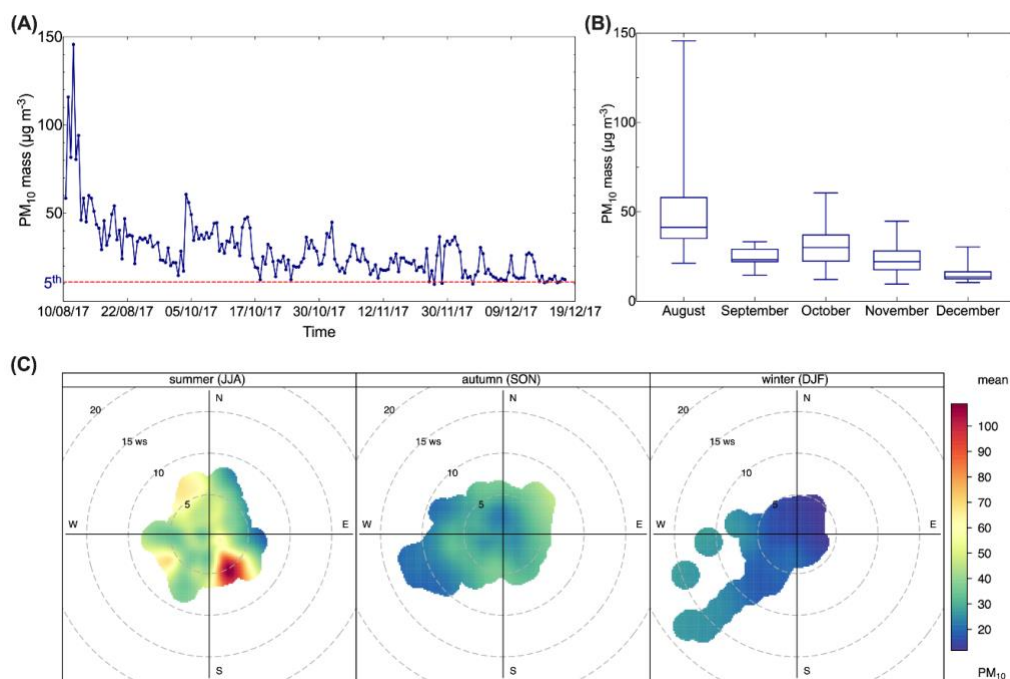


Figure 3. (A, top right) Time series of daily PM₁₀ mass; (B, top left) Box plot of monthly averages of PM₁₀ mass; (C, bottom) Pollution rose of PM₁₀ mass; The presented data were separated according to each season into summer (Aug), Fall (Sep-Nov), and winter (Dec).

R1-C12: Maybe the authors could shorten and reorganize the paper as NAO+MCE (as they are similar); ACE; SD; and local remote/background - these are perhaps more interesting for atmospheric research and future campaign planning than monthly data.

R1-A12: We thank the reviewer for his suggestion to reorganize the air mass classification section. Accordingly, the manuscript has been organized according to the reviewer's suggestion, the NOA and ACE air masses have been grouped, and Background Air masses; (BAM) have been introduced in the classification. Figure 4 has been modified as follows:

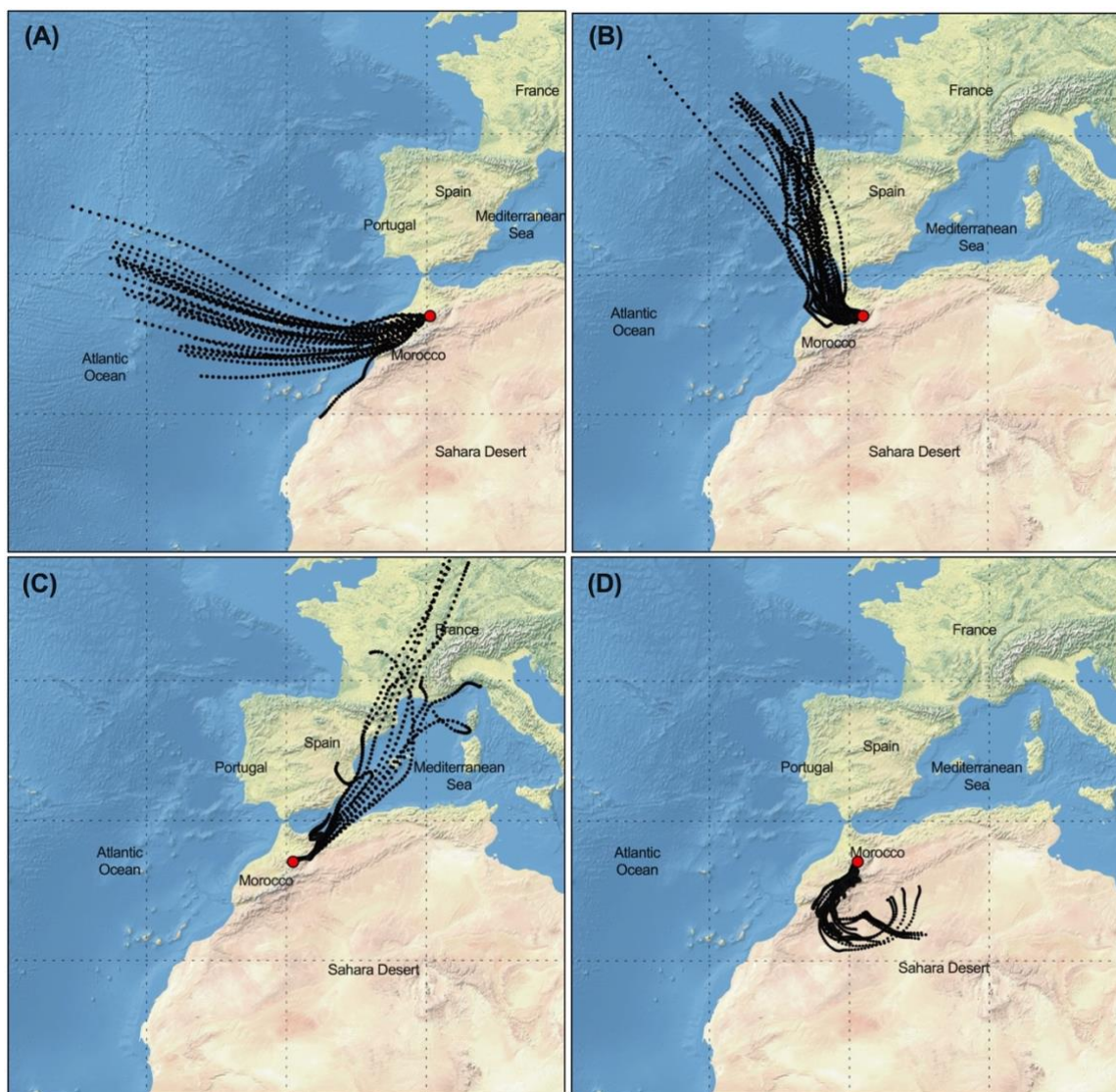


Figure 4. Typical 96h air mass back trajectory performed for AM5 during routine samples periods; aerosol type and PM_{10} mass concentration are given in parentheses: (a) 18 December 2017: air mass from the North Atlantic Ocean considered to be representative of background conditions (Background, $m=10.9 \mu\text{g m}^{-3}$); (b) 10 October 2017: air mass from Europe crossing coastline of North Morocco (Atlantic Coast Europe, $m=44.1 \mu\text{g m}^{-3}$); (c) 2 November 2017: slightly polluted air mass from North East crossing Mediterranean Sea (Mediterranean Coast Europe, $m=26.4 \mu\text{g m}^{-3}$); (d) 13 August 2017: dust loaded air mass coming from Sahara desert (Saharan Dust, $m=94.1 \mu\text{g m}^{-3}$).

The paragraph describing the results of updated air mass classification in section air mass origins (3.2) has been modified. The corresponding sentences have been modified in lines 347-357 as follow and now read:

“The calculation of back trajectories using the Hysplit model allowed the identification of several remote sources of PM₁₀ at the station. Four main air masses categories were identified as shown in Fig. 4. i) Air masses that spent the last 96h over the Atlantic Ocean at high-altitude (1000 m.asl), representative of typical background air mass (BAM) conditions, which influenced about 5.3% of all samples; ii) Air masses originating from the Atlantic and crossing over the Coast of Europe (ACE), especially Spain and over Moroccan industrial cities located at the North Atlantic coast, influencing about accounts 26.8% of all samples; iii) Air masses from Europe crossing over the Mediterranean Coast and Europe (MCE) as well as over North Moroccan cities, as shown in Fig. 4c and influencing about 37.4% of all samples and iv) Air masses originating from Southern and/or Eastern Sahara crossing the desert (SD), at different altitudes before arriving at the AM5 and influencing about 22.6% of all samples. The remaining back trajectories represent mixing scenarios including 7.9% of all samples that could not be assigned to the four major classes mentioned above.”

Consequently, the chemical composition corresponding to each air mass has been modified, as presented in Table 4. The concentrations of the compounds have been modified according to the new classification.

Table 4. PM₁₀ concentrations ($\mu\text{g m}^{-3}$) of main aerosol chemical species according to the air mass influence at AM5; The organic composition is given in ng m^{-3} ; The number of samples is written in parentheses.

Aerosol components	Air mass			
	BAM (n=10)	ACE (n=51)	MCE (n=71)	SD (n=43)
Mass load	10.9 ± 0.9	20.4 ± 6.3	33.8 ± 14.5	37.9 ± 25.3
Dust	5.5 ± 3.5	13.3 ± 5.2	19.9 ± 11.9	29.1 ± 22.6
Sea salt	0.05 ± 0.06	0.3 ± 0.5	0.3 ± 0.4	0.2 ± 0.2
OM	1.0 ± 0.6	1.4 ± 1.1	2.7 ± 1.7	2.3 ± 1.8
EC	0.2 ± 0.1	0.2 ± 0.1	0.2 ± 0.1	0.2 ± 0.1
POC	0.1 ± 0.06	0.2 ± 0.3	0.3 ± 0.3	0.2 ± 0.2
SOC	0.3 ± 0.2	0.4 ± 0.4	1.0 ± 0.8	0.9 ± 0.8
NO ₃ ⁻	0.5 ± 0.6	0.6 ± 0.7	1.0 ± 0.7	0.9 ± 0.4
nss-SO ₄ ²⁻	0.2 ± 0.2	0.5 ± 0.5	1.2 ± 0.9	1.0 ± 0.6
NH ₄ ⁺	0.2 ± 0.2	0.2 ± 0.2	0.3 ± 0.2	0.2 ± 0.1
Ca ₂ ⁺	0.2 ± 0.2	0.2 ± 0.2	0.8 ± 0.5	0.9 ± 0.6
Alkanes	4.9 ± 3.2	5.6 ± 3.7	10.5 ± 7.7	9.2 ± 8.6
PAHs	0.4 ± 0.5	0.4 ± 0.4	0.9 ± 2.1	0.7 ± 0.7
Alkan-2-ones	7.8 ± 6.9	5.9 ± 5.5	5.5 ± 5.0	6.6 ± 4.1
Sugars	-	3.7 ± 6.0	5.2 ± 7.7	1.8 ± 2.9
Oxalate	44 ± 26	73 ± 58	129 ± 58	107 ± 63
pH	5.6 ± 0.2	6.0 ± 0.4	6.5 ± 0.4	6.5 ± 0.4
OC/EC	2.2 ± 1.1	3.3 ± 1.9	6.3 ± 7.5	4.6 ± 4.6
CPI	3.3 ± 0.8	3.5 ± 2.4	3.9 ± 1.9	4.0 ± 3.1

The comparison between the chemical composition with respect to the air masses (Table 4) has been included in the discussion paragraphs in section (3.3). The corresponding sentences have been added as follow:

In lines 383-389: “Mineral dust was found to be more than 7 times higher ($37.9 \pm 25.3 \mu\text{g m}^{-3}$) during dust events (SD), in comparison to remote background conditions (BAM) with an average concentration of $5.5 \pm 3.5 \mu\text{g m}^{-3}$, as observed in Table 4. Other less intense Saharan dust storms occurred during the summer season between the 21st and 24th of August with a similar high dust concentration that was 5 times higher than dust background concentrations. The presence of mineral dust is relatively low but still significant for air masses other than SD, such as during the ACE ($13.3 \pm 5.2 \mu\text{g m}^{-3}$) and MCE ($19.9 \pm 11.9 \mu\text{g m}^{-3}$) air mass influence, as shown in Table 4.”

In lines 444-445: “The highest OC/EC ratio (6.3 ± 7.5) was observed for MCE air masses, while the lowest ratio was recorded for BAM at about 2.3 ± 1.1 , as shown in Table 4.”

In lines 462-463: “However, no significant difference was noticed in sea salt concentrations found in the ACE ($0.5 \pm 0.7 \mu\text{g m}^{-3}$) and MCE samples ($0.5 \pm 0.5 \mu\text{g m}^{-3}$), as shown in Table 4.”

In lines 494-496: “On average, the influence of long-range transport during the ACE and MCE air masses for sulfate ($2.8 \mu\text{g m}^{-3}$) and nitrate ($2.3 \mu\text{g m}^{-3}$) were similar. However, the contribution of ammonium ($1.7 \mu\text{g m}^{-3}$) to particulate matter was particularly higher for MCE air mass.”

In lines 550-552: “Table 4 presents the CPI values calculated according to each air mass. The average CPI value was 3.8 ± 2.4 and ranged from 0.7 to 18.6. However, high CPI ($\gg 1$) was observed for all air masses, which indicates that the alkanes originated from plants waxes, as presented in Table 4 (Kavouras, 2002).”

In lines 570-575: “The highest amount of PAH was detected during October, approximately 5.7 ng m^{-3} due to long-range transport of MCE air masses, as shown in Figure 6. The minimum concentration was observed during winter, of about 0.05 ng m^{-3} . The average background concentration of PAHs was $0.4 \pm 0.5 \mu\text{g m}^{-3}$, which was low in comparison to other organic compounds likely because of high evaporation on warm days (Cincinelli et al., 2007). During MCE air mass, the PAH concentrations increased by 52% compared to the BAM concentration, as shown in Table 4.”

In lines 630-641: “The average sugar concentrations during these air mass influences were ACE ($3.7 \pm 6.0 \text{ ng m}^{-3}$) and MCE ($5.2 \pm 7.7 \text{ ng m}^{-3}$), as listed in Table 4. In contrast, sugar compounds were relatively low in SD ($1.8 \pm 2.9 \text{ ng m}^{-3}$) air masses and were not found in the background PM_{10} conditions. Levoglucosan which is considered as a good tracer of biomass burning emissions in aerosol particulate matter, was particularly higher for ACE (2.0 ng m^{-3}) and MCE (1.6 ng m^{-3}) air mass influence, as displayed in Fig. S8. (Bauer et al., 2008). Arabitol shows a similar concentration for MCE and ACE with a mean of 1.0 ng m^{-3} suggesting that particles were loaded with primary biological aerosols such as pollen, fungal spores, vegetative debris, viruses, and bacteria from the marine coast (Fu et al., 2012). Glucose remained relatively high during MCE air mass influence in comparison to other air masses influence. During SD air mass influence, the concentration of arabitol was extremely low with a concentration less than 0.08 ng m^{-3} . However, glucose showed a higher concentration of about 0.7 ng m^{-3} but remains 3 times lower than MCE concentrations. This indicates that the sugars were most likely originated from marine air masses.”

The background shading type has been modified to improve visibility. Thus, each sample is represented by a distinguishing color symbol for each specific air mass. At the same time, Figure 6, which shows the temporal variation of the organics, has been modified in the same way. The new Figure 5 and Figure 6 are shown below:

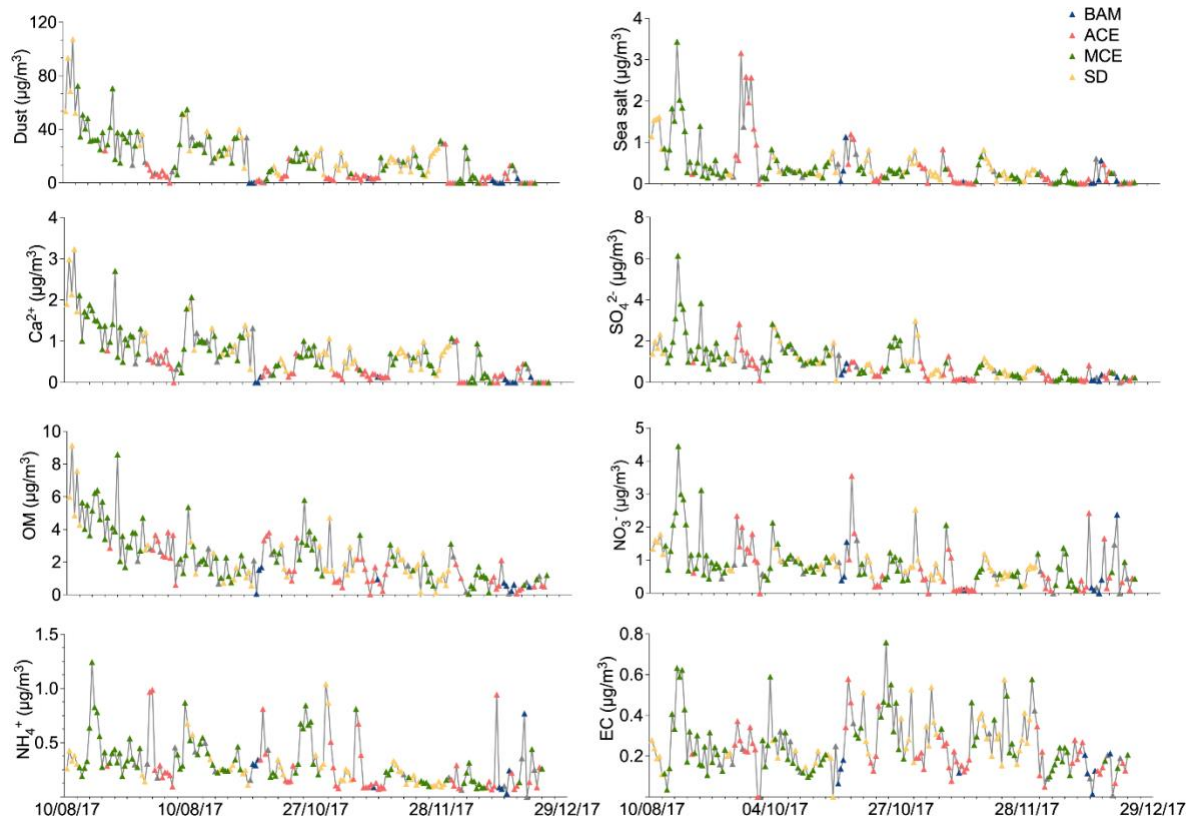


Figure 5. Time series of major aerosol chemical constituents in PM₁₀ filter samples collected from August to December 2017; The color of the symbols displayed for each sample represents a specific air mass origin: Background (blue); ACE (red); MCE (green); SD (yellow).

Consequently, the description of Figure 5 has been modified in section 3.3 according to the new air mass classification, so the modified paraphrases are listed as follows:

In lines 364-368: "During the 5 months of PM collection at the AM5 site, the average mineral dust concentration was about $17.7 \pm 7.4 \mu\text{g m}^{-3}$ and varied strongly between $0.05 \mu\text{g m}^{-3}$ and $107 \mu\text{g m}^{-3}$. The highest mean concentrations were observed in August ($39 \mu\text{g m}^{-3}$) and the lowest in December ($3.7 \mu\text{g m}^{-3}$). Low concentrations were observed during days with low wind speeds ($< 2 \text{ m s}^{-1}$), low Saharan dust air mass inflow, and after precipitation events, which typically occurred in the fall and winter."

In lines 404-415: "Organic carbon (OC) and elemental carbon (EC) showed strong variation and distinct differences with an average of $1.1 \pm 0.8 \mu\text{g m}^{-3}$ and $0.2 \pm 0.1 \mu\text{g m}^{-3}$, respectively. The OC has both primary and secondary origin, and can be formed from primarily emitted substances through condensation or chemical reactions among them (Sarkar et al., 2019). The OC concentration reached a maximum $4.5 \mu\text{g m}^{-3}$ during summer, whereas the lowest concentration was observed during winter at about $0.03 \mu\text{g m}^{-3}$. The average concentration of OC progressively decreased from summer ($2.1 \pm 0.8 \mu\text{g m}^{-3}$) to winter ($0.3 \pm 0.2 \mu\text{g m}^{-3}$). The abundant contribution of organic matter in summer can be due to high biogenic emissions in the Middle Atlas. A slight increase in OC was also observed during dust events, as shown in Fig. 5, which suggests that the dust deposited at AM5 also contained biogenic material from the surroundings of the Middle-Atlas region."

In lines 464-469: "The Middle Atlas region is influenced by two maritime sources of sea salt, more often from the Atlantic Ocean, and sometimes from the Mediterranean Sea. During the study period, the average concentration of sea salt remains low ($0.45 \pm 0.55 \mu\text{g m}^{-3}$) and contributed only 1.6% of the total PM_{10} concentration. The highest concentrations were recorded during August when sea salt concentrations reached a maximum of $3.4 \mu\text{g m}^{-3}$. The sea salt then decreased gradually, reaching a minimum concentration of $0.06 \mu\text{g m}^{-3}$ during December. The sea salt concentration was high when wind speed exceeded 6 m s^{-1} , indicating that sea salt is strongly dependent on meteorological conditions and air mass sources."

In lines 487-498: "A significant part of PM composition was associated with the formation of secondary inorganic aerosols (SIA), which are mainly composed of sulfate, nitrate, and ammonium. They made up about 7.2% of the PM_{10} mass. The temporal variation during the sampling period of SO_4^{2-} , NO_3^- , and NH_4^+ is presented in Fig. 6, with average concentrations of $0.9 \pm 0.8 \mu\text{g m}^{-3}$, $0.8 \pm 0.6 \mu\text{g m}^{-3}$, and $0.3 \pm 0.2 \mu\text{g m}^{-3}$, respectively. In summer, the concentrations were relatively high during few days in August, with the observation of the highest sulfate, nitrate, and ammonium concentrations of up to $6.1 \mu\text{g m}^{-3}$, $4.4 \mu\text{g m}^{-3}$, and $1.2 \mu\text{g m}^{-3}$, respectively (Fig. 6). This was due to the transport of polluted MCE air masses through the Mediterranean Sea and across cities in the North of Morocco leading to high PM loaded aerosols. On average, the influence of long-range transport during the ACE and MCE air masses for sulfate ($2.8 \mu\text{g m}^{-3}$) and nitrate ($2.3 \mu\text{g m}^{-3}$) were similar. However, the contribution of ammonium ($1.7 \mu\text{g m}^{-3}$) to particulate matter was particularly higher for MCE air mass. Additionally, other peaks were also observed in aerosol concentrations both for SO_4^{2-} and NO_3^- during August. This could be attributed to the long-range transport of dust aerosol from the Saharan desert in Southern Morocco. The subsequent months demonstrate a clear decreasing trend of SIA from high concentrations in summer ($3.8 \mu\text{g m}^{-3}$), to relatively low concentrations during winter ($1.0 \mu\text{g m}^{-3}$)."

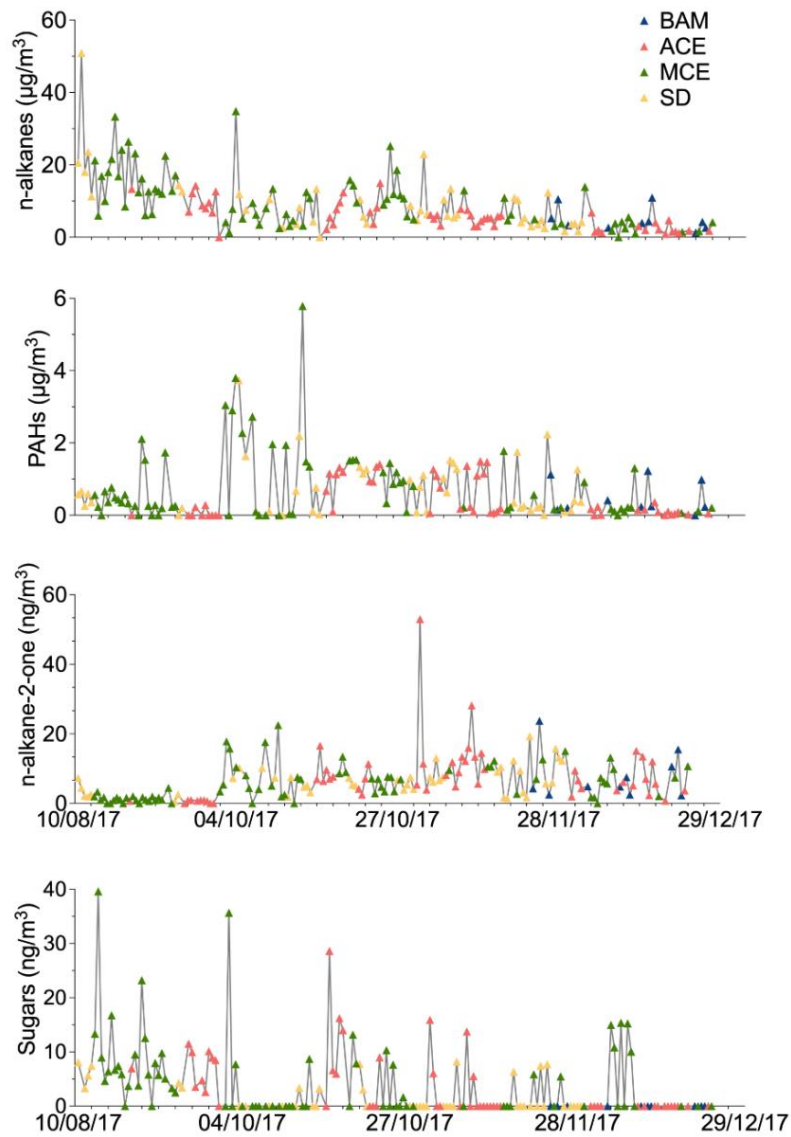


Figure 6. Time series of organic compounds in PM_{10} filter samples collected from August to December 2017 at AM5; The color of the symbols displayed for each sample represents a specific air mass origin: Background (blue); ACE (red); MCE (green); SD (yellow).

The description of Figure 6 has been modified in the section of the organic compound (3.3.5) in line with the new air mass classification, so the modified lines are listed as follows:

In lines 529-533: "The distinguishing aspect of alkanes is their specific source and their ability to provide information about their origins (Pietrogrande et al., 2010). Individual n-alkanes with C-atom numbers in the range 19-34 were analyzed. Figure 6 shows the temporal variation of the n-alkanes revealing strong variations over the seasons with an average concentration of about $8.4 \pm 7.1 \text{ ng m}^{-3}$. The average concentration decreases from summer ($16.1 \pm 8.9 \text{ ng m}^{-3}$) to winter ($2.6 \pm 2.0 \text{ ng m}^{-3}$)."

In lines 566-572: "In the present study, polycyclic aromatic hydrocarbons (PAHs) with 3 to 7 rings were quantified. The temporal variation of the sum of the 20 identified PAH compounds in the particle is presented in Figure 6. The contribution of PAHs remains much lower than alkanes with an average concentration of $0.7 \pm 0.8 \text{ ng m}^{-3}$ over the whole study period. Contrary to what has been observed for alkanes, the PAH concentrations determined during the autumn months are higher than those during the summer and winter. The highest amount of PAH was detected during October, approximately 5.8 ng m^{-3} due to long-range transport of MCE air masses, as shown in Figure 6. The minimum concentration was observed during winter, of about 0.05 ng m^{-3} ."

In lines 590-598: "In total, 5 n-alkan-2-ones were detected in this study, as shown in Fig .S8. The n-alkan-2-one concentrations increased significantly from summer (1.8 ng m^{-3}) to autumn (9.7 ng m^{-3}), then decreased continuously to winter (6.3 ng m^{-3}), with an average of 6.6 ng m^{-3} for the whole sampling period. The minimum concentration was recorded during the summer of about 0.60 ng m^{-3} . In contrast, the maximum concentration was reached during autumn of about 52 ng m^{-3} due to ACE air mass influence, as shown in Fig. 6. The sum of n-alkan-2-one was between 0.67 to 13.2 ng m^{-3} . The same relative composition of n-alkan-2-one concentrations was observed in both seasons, suggesting that they came from similar sources. However, the levels of n-alkan-2-one were much lower in concentration than those of n-alkanes. The average background concentration of the total n-alkan-2-one was $5.9 \pm 5.5 \text{ ng m}^{-3}$."

Further comments

After restructuring the manuscript to improve readability and logical flow (and some light copy-editing*) the paper can be re-reviewed and considered suitable for publication.*Some examples:

R1-C13: Lines 160-161: please use either km/h or m/s, but not both especially when comparing two values.

R1-A13: The unit “ $m s^{-1}$ ” was used to describe the wind speed and has been used to replace $km h^{-1}$ throughout the whole manuscript. The sentences can be read as follow:

Lines 149-150: “The average wind speed at AM5 was about $5.8 m s^{-1}$ but reached a maximum of $19.7 m s^{-1}$ due to turbulence in the mountain region, especially during winter.”

Line 150: “Over the summer, the minimum wind speed was about $1.6 m s^{-1}$, and the relative humidity (RH) was low.”

Lines 163-164: “During summer, southeast winds have a higher frequency but a lower average speed of about $5.8 m s^{-1}$.”

Lines 165-166: “During this period, there is a strong occurrence of westerly winds which are often characterized by high wind speeds (stiff breeze) of up to $20 m s^{-1}$.”

Lines 299-300: “For example, PM_{10} mass concentration often exceeded $50 \mu g m^{-3}$ and sometimes even reached up to $145 \mu g m^{-3}$ during August, when the wind speed was stronger than $9 m s^{-1}$.”

Lines 306-307: “High PM_{10} concentrations were observed during strong westerly winds of up to $> 7 m s^{-1}$.”

Lines 320-321: “The samples within this PM concentration range were had similar air mass trajectories and typical meteorological conditions with low wind speeds $< 3 m s^{-1}$.”

Lines 336-438: “Low concentrations were observed during days with low wind speeds ($< 2 m s^{-1}$), low Saharan dust air mass inflow, and after precipitation events, which typically occurred in the fall and winter.”

Lines 457-459: “The sea salt concentration was high when wind speed exceeded $6 m s^{-1}$, indicating that sea salt is strongly dependent on meteorological conditions and air mass sources.”

Lines 800-801: “High speeds were recorded during the night, up to $17.5 m s^{-1}$, mostly associated with marine air masses.”

R1-C14: It is unclear why low wind speeds indicate Saharan dust reaches AM5 via this path.

R1-A14: The change in wind direction in addition to the wind speed is responsible for the transport of the Saharan dust. Nevertheless, the low wind speed from the south recorded during summer is due to the High Atlas Mountains which protect the site and act as a barrier to block the transport of Saharan mineral dust. By contrast, the marine air masses coming from the west are characterized by strong winds and can reach maximum speeds of $20 m s^{-1}$. As result, the sentences have been corrected in section 3.3.1 in lines 368-375, and now read:

“The influence of the Saharan dust on the Middle Atlas region remains relatively dependent on meteorological conditions. Firstly, the direction and speed of the wind, as the typical Saharan dust events were observed during high wind speed periods from south and southeast. Secondly, their progression depends mainly on favorable weather conditions for transport, the difference in temperature between day and night, humidity, and especially the scarcity of rainfall. Thirdly, the High-Atlas mountains situated at 4000 m of altitude acts as a barrier to

Saharan dust transport which forces the winds to deviate from their path. All these factors influence the transport of large particles from the Sahara to the Middle-Atlas during the different seasons.”

RI-C15: Also the authors say summer is dominated by southwestern winds, but only describe westerly and southeasterly winds.

RI-A15: The polar rose of PM_{10} in Figure 3c has been modified accordingly for each month to discuss the variation of PM_{10} concentration with respect to wind speed and direction. A description of southwestern winds has been added in lines 305-307, and now reads:

“Furthermore, high concentrations up to $40\text{-}50 \mu\text{g m}^{-3}$ were observed as well with westerly winds, especially during northwest and southwest winds. The highest PM_{10} concentrations was observed during strong westerly winds of up to $> 7 \text{ m s}^{-1}$.”

RI-C16: The last sentence of this section then says summer is dominated by southern winds, so this section is also confusingly structured/worded.

RI-A16: The last sentence of the section has been deleted and the paragraph has been restructured and rewritten, and the lines 298-316 now read:

“During August, the high PM_{10} concentrations were mostly related to high wind speeds from the southeast. For example, PM_{10} mass concentration often exceeded $50 \mu\text{g m}^{-3}$ and sometimes even reached up to $145 \mu\text{g m}^{-3}$ during August, when the wind speed was stronger than 9 m s^{-1} . The high PM_{10} concentration recorded was due to the influence of Saharan dust events during periods of air mass influence from the southern sector located in the southeast of the AM5 station. The Middle Atlas region is marked by particular meteorological conditions during the summer with low humidity and often low precipitation (avg. 37 mm), as shown in Table 1. These hot and arid conditions are known to favor the transport of dust particles from the Saharan desert to the Atlas Mountains (Rodríguez et al., 2011). Furthermore, high concentrations of up to $40\text{-}50 \mu\text{g m}^{-3}$ were observed as well with westerly winds, especially during northwest and southwest winds. High PM_{10} concentrations were observed during strong westerly winds of up to $> 7 \text{ m s}^{-1}$. The back trajectory analysis suggests that the high concentrations during this period were most likely associated with the long-range transport of aerosol particles from the western coast of the Iberian Peninsula. In contrast to the summer period, PM_{10} mass concentrations were lower during the fall, despite some temporal peaks. The PM_{10} concentrations were generally lower in September ($24.2 \pm 5.1 \mu\text{g m}^{-3}$) and October ($30.5 \pm 10.8 \mu\text{g m}^{-3}$). During this period, winds originated from the northeast suggesting the influence of air mass transport from the Mediterranean Sea coast. A sharp fall in PM concentrations was noticed in November ($22.8 \pm 7.9 \mu\text{g m}^{-3}$) and December ($15.9 \pm 5.6 \mu\text{g m}^{-3}$). Overall, PM_{10} concentration decreased from the summer to winter by 32%. This trend is most likely due to the increased amount of precipitation (peaks of 852mm) during fall and winter, which can lead to the wash-out effect of aerosol and its components (Holst et al., 2008).”

Figure 7 has been updated according to the new air mass classification. The category of Background Air Masses has been added as follow:

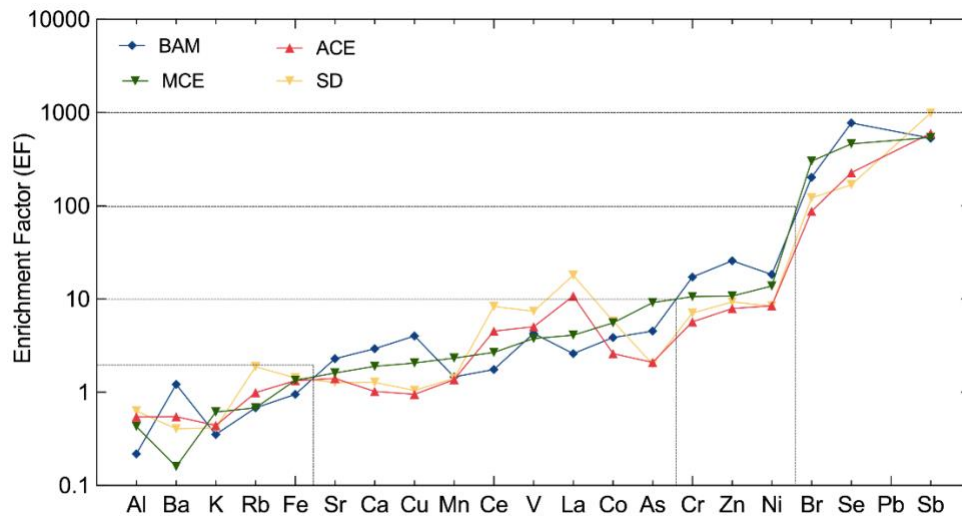


Figure 7. Crustal enrichment factors (EF) of aerosol PM_{10} evaluated for the different trace metal elements at AM5; The averaged values are plotted according to their respective air mass origins.

The correlation plot displayed in Figure 8 have been updated according to the new air mass classification as follow:

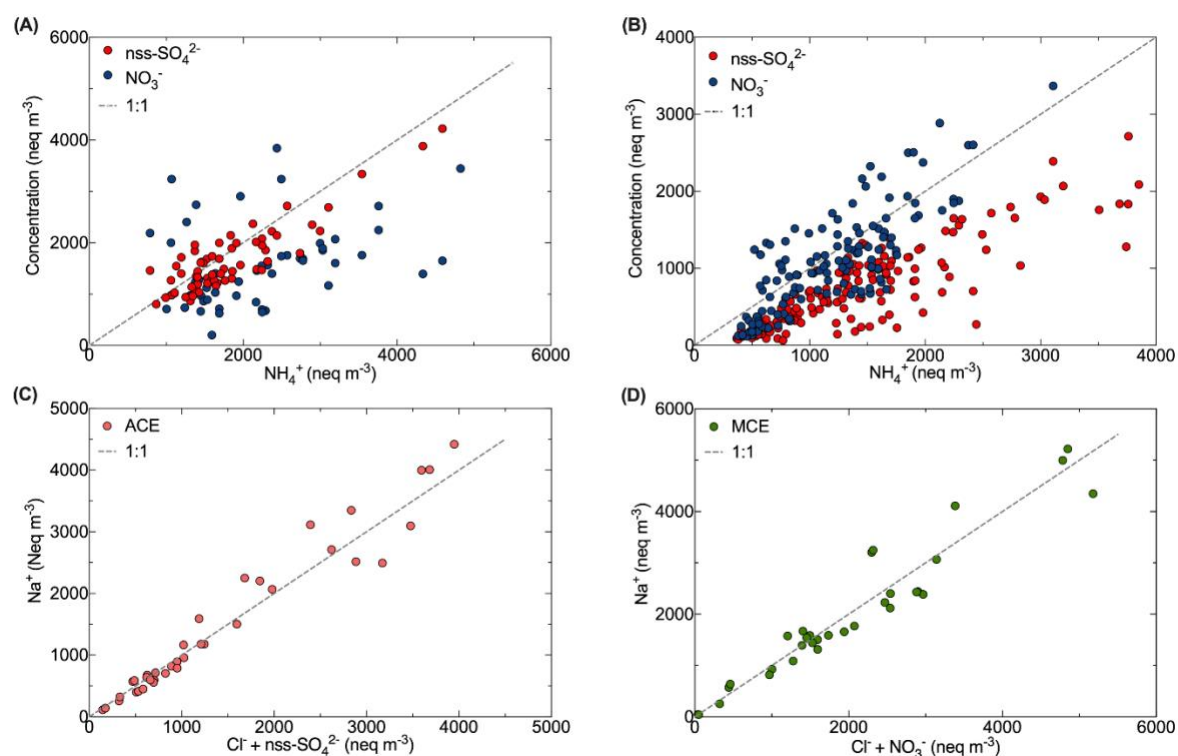


Figure 8. Scatter plot of (A) NH_4^+ with NO_3^- and nss-SO_4^{2-} during summer; (B) NH_4^+ with NO_3^- and nss-SO_4^{2-} during autumn-winter; (C) Na^+ and $\text{Cl}^- + \text{SO}_4^{2-}$ during ACE air mass; (D) Na^+ and $\text{Cl}^- + \text{NO}_3^-$ during MCE air mass at the AM5 site.

The inter-relationship between aerosol components section (3.4) has been restructured by adding subheadings as follow:

3.4.1 Nitrate and nss-sulfate

3.4.2 Ammonium nitrate and ammonium sulfate

3.4.3 Sodium and chlorine

Therefore, the discussion paragraphs of different correlations have been reformulated as follow:

In lines 708-721: "The correlation between NO_3^- and nss-SO_4^{2-} ($r^2=0.76$) indicates their possible common origin. The correlation was more pronounced for MCE air masses ($r^2=0.80$) in contrast to ACE ($r^2=0.43$) air masses, suggesting an enhanced transport of secondary anthropogenic aerosol from the Mediterranean coast (Liu et al., 2017) to the AM5 site. The nss-sulfate concentrations were slightly correlating with Vanadium which is associated with the emissions of oil combustion, ship emissions as well as iron and steel industrial emissions (Pandolfi et al., 2011). A strong correlation of NO_3^- and nss-SO_4^{2-} was observed with oxalate ($\text{C}_2\text{H}_4^{2-}$), which could indicate that

they have a common source and that they can originate from biomass burning and secondary transformations. Nss-SO_4^{2-} also originated from crustal sources especially as elevated concentrations were observed during dust events. This assertion was supported by a good correlation of nss-SO_4^{2-} with nss-Ca^{2+} (Fig. S7), indicating the likely presence of calcite particles of crustal origin. A similar observation was reported by [Okada and Kai, \(2004\)](#), who observed that Desert dust was associated with sulfur compounds and organic matter from surrounding agricultural areas. Indeed, the particles with high sulfate content were accompanied by Ca and were assigned as gypsum particles, also suggesting that the sulfur in these particles originated from a sedimentary source ([Falkovich et al., 2001](#)).”

In lines 728-741: “The analysis of the correlation matrices between nss-SO_4^{2-} and NO_3^- with ammonium (NH_4^+) was applied to better understand the inter-relationship between the secondary inorganic species. A correlation between nss-SO_4^{2-} and NH_4^+ ($r^2= 0.90$) supported the hypothesis of dominant ammonium sulfate particles ($\text{NH}_4)_2\text{SO}_4$ in the summer especially when air masses were coming from ACE, as shown in Fig. 8. During this period, a strong correlation was found between sulfate and solar radiation which suggests that nss-SO_4^{2-} was produced via photochemical reaction ([Baker and Scheff, 2007](#)). Nevertheless, the transport of nss-SO_4^{2-} from the Atlantic coast also contributes to the formation of ammonium sulfate. However, the trend is more towards ammonium nitrate (NH_4NO_3) in winter, given that the main correlation of NH_4^+ with NO_3^- ($r^2= 0.95$) mainly present in MCE air masses. Nitrate shows a strong dependency on the temperature at AM5, most likely due to the stability of ammonium nitrate in the atmosphere at low temperatures ([Squizzato et al., 2013](#)). The predominance of nitrates over sulfates during winter, where nitrates and ammonium remain high, is probably due to the influence of temperature that prevents the dissociation of ammonium nitrate particles ([Ricciardelli et al., 2017](#)). Moreover, a similar pattern of NO_3^- and NH_4^+ as observed by [Querol et al., 2004](#) in the Mediterranean coast with a summer minimum and suggested that it could be due to the low thermal stability of the nitrate in the hot season.”

In lines 738-750: “The evolution of the sea salt constituents and their relationship with the most important aerosol acidic species such as NO_3^- and SO_4^{2-} was investigated according to their air mass origins (Fig. 8). A correlation between sodium and chlorine was observed ($r^2=0.76$), as shown in Fig. 8. The scatter plot of molar equivalent concentrations of Na^+ and Cl^- shows a strong correlation specifically for ACE and SD air masses. However, the data points are below the seawater reference line and only approach this line when the Cl^- concentration is combined with NO_3^- and nss-SO_4^{2-} . This indicates that chloride was depleted in the sea salt particles due to the displacement of chloride by sulfate from sulfuric acid when air masses were coming from MCE and ACE, especially as photochemical processes favor sulfate formation during summer. The same scenario has been observed for NO_3^- with a considerable difference during the winter. Indeed, the correlation between sodium and the sum of chloride and nitrate shows the chloride depletion and indicates that the Mediterranean Sea air mass was loaded with aged sea salt. Similar results were observed in the North of Morocco where the mass fraction of nitrate was higher in the coarse fraction which indeed corresponds to aged sea salt ([Benchrif et al. 2018](#)). No correlation between Na^+ and Cl^- was observed in the BAM conditions.”

R1-C17: Line 260: Either delete "while" or replace it with "However" or combine this sentence with the previous sentence - separating the two as "mineral dust, while...".

R1-A17: "While" was deleted and replaced by "However" in Lines 262-263, and now reads:

"However, method 2 allows to take into account the overall mineral composition and therefore was applied in this study."

R1-C18: Line 293: replace "accordingly" with "for example,"

R1-A18: The word "accordingly" was replaced with "for example,"

The corresponding sentence has been modified on lines 298-300, which now reads:

"During August, the high PM₁₀ concentrations were mostly related to high wind speeds from the southeast. For example, PM₁₀ mass concentration often exceeded 50 µg m⁻³ and sometimes even reached up to 145 µg m⁻³ during August, when the wind speed was stronger than 9 m s⁻¹."

R1-C19: Line 294: says PM₁₀ peaked at 143 µg/m³ but line 307 says the peak was 145 µg/m³.

R1-A19: The corresponding PM₁₀ concentration has been corrected. The corresponding sentence has been modified on lines 289-290, which now reads:

"The PM₁₀ mass concentration time series at the AM5 station varied from 9.5 µg m⁻³ to 145.6 µg m⁻³ with averaged of 29.2 ± 17.3 µg m⁻³."

R1-C20: Line 336: delete "In contrast" (and in any case, probably don't compare AM5 to a complex urban site outside Morocco as mentioned earlier.)

R1-A20: The comparison with other urban sites has been removed and replaced by urban Moroccan sites. In addition, the term „In contrast“ was deleted.

R1-C21: Lines 348-349: I assume they mean the urban sites in Morocco are twice or thrice (not trice; also, "two or three times" is better) the AM5 values, but the sentence is unclear.

R1-A21: Indeed, a typing error was made in the sentence. Therefore the sentence has been rephrased in lines 340-343, and now reads:

“Other Moroccan sites, such as Marrakech, Meknes, and Agadir, which are exposed to strong urban emissions, usually show PM₁₀ concentrations between 50 and 110 µg m⁻³, which is much higher than the concentration found at AM5 in this study (Inchaouh et al., 2017; Tahri et al., 2012; Tahri et al., 2017).”

R1-C22: The first two sentences of this paragraph could be easily rephrased as "Urban sites show PM10 values two to three times that observed at AM5 (Table 3)." However, I just noticed only one other site in Morocco listed in Table 3 - Tetouan, which has very similar PM₁₀ to AM5.

R1-A22: In addition to the Tetouan site, other Moroccan sites such as Marrakech, Kenitra, and Meknes, have now been added in Table 3 as presented previously. Therefore, the sentences in lines 340-345 have been revised and now read:

“Other Moroccan sites, such as Marrakech, Meknes, and Agadir, which are exposed to strong urban emissions, usually show PM₁₀ concentrations between 50 and 110 µg m⁻³, which is much higher than the concentration found at AM5 in this study (Inchaouh et al., 2017; Tahri et al., 2012; Tahri et al., 2017). These results highlight a better air quality at AM5 in comparison to many sites and indicate that the station can serve as a good remote reference station for defining background concentrations in Morocco and possibly the whole of North Africa.”

References

Escudero, M., Stein, A., Draxler, R. R., Querol, X., Alastuey, A., Castillo, S., and Avila, A.: Determination of the contribution of northern Africa dust source areas to PM₁₀ concentrations over the central Iberian Peninsula using the Hybrid Single-Particle Lagrangian Integrated Trajectory model (HYSPLIT) model, *J. Geophys. Res.*, 111, D06210, <https://doi.org/10.1029/2005JD006395>, 2006.

Harrison, R. M., Jones, A. M., and Lawrence, R. G.: Major component composition of PM₁₀ and PM_{2.5} from roadside and urban background sites, *Atmospheric Environment*, 38, 4531–4538, <https://doi.org/10.1016/j.atmosenv.2004.05.022>, 2004.

Karaca, F., Anil, I., and Alagha, O.: Long-range potential source contributions of episodic aerosol events to PM₁₀ profile of a megacity, *Atmospheric Environment*, 43, 5713–5722, <https://doi.org/10.1016/j.atmosenv.2009.08.005>, 2009.

Puxbaum, H., Gomiscek, B., Kalina, M., Bauer, H., Salam, A., Stopper, S., Preining, O., and Hauck, H.: A dual site study of PM_{2.5} and PM₁₀ aerosol chemistry in the larger region of Vienna, Austria, *Atmospheric Environment*, 38, 3949–3958, <https://doi.org/10.1016/j.atmosenv.2003.12.043>, 2004.

Vardoulakis, S. and Kassomenos, P.: Sources and factors affecting PM₁₀ levels in two European cities: Implications for local air quality management, *Atmospheric Environment*, 42, 3949–3963, <https://doi.org/10.1016/j.atmosenv.2006.12.021>, 2008.

We thank referee #2 for the many constructive comments and suggestions which helped to improve the manuscript. To improve readability, we numbered each reviewer comment and its corresponding response in the style R2-C1 for reviewer 2 comment 1 and R2-A1 for reviewer 2 answer to comment 1, respectively. Comments by the reviewer are given in black, our response to the comments are shown in red, and modified text in the revised manuscript are given in green. Supporting information (SI) has been added. In the following, we provide a point-by-point response to all comments.

In the following, we provide a point-by-point response to all comments.

RC2: 'Comment on acp-2021-106', Anonymous Referee #3, 11 Jul 2021

R2-C1: This paper presents results from 12-hour PM₁₀ filter samples taken on a newly established high-altitude site (AM5) in Morocco in the middle Atlas. The filters were analyzed for inorganic and organic constituents of particulate matter. The analysis takes into account the meteorological situation like backward trajectories and wind speed. Such data sets are very important for the scientific community, because information on aerosol composition at such remote sites are sparse. The technical aspects of filter analysis are not my field of expertise, but I believe that such a well know institute as TROPOS knows very well how to conduct filter analysis properly. Overall I think the manuscript deserves publication, although I have some concerns about the further data analysis (after the chemical analysis of the filters) and presentation of the results. Since my suggestions include re-structuring of the manuscript, I list them as “major revisions”:

R2-A1: The manuscript has been copy-edited and large parts of the manuscript have been thoroughly improved. Figures have been improved. Grammatic errors have been corrected and the language has been edited to be more concise throughout. The references have been edited to avoid errors in the citations. The structure of the manuscript has been improved. The classification criteria have been reconsidered, therefore some of the results have been modified. Some sections have been combined to improve readability, comparisons, and avoid repetition.

A point-by-point description of the changes made to the manuscript is listed in the following.

R2-C2: I suggest to re-structure the results section as follows: Start with 3.1 (Variation of PM10 mass), then continue with 3.4. (Characterization of aerosol chemical composition for the complete measurement period). Then 3.3 (Air mass classification), then 3.7. (day-night), then 3.6 (dust vs non-dust) and only then 3.2 (Aerosol composition under remote background conditions). Thus, I mean ordering the sections from “robust classification” down to “less well-defined” classification.

R2-A2: The results section has been restructured according to the following proposed structure. However, the classification of air masses (3.3) was interchanged with the characterization of Aerosol chemical composition of the complete measurement period (3.4) to facilitate the referencing to the air mass history. Furthermore, as also suggested by the other reviewer (R1-C12), the background conditions have been considered as a separate air mass category. Consequently, its discussion has been incorporated into that of the updated air mass classification (3.3) and the characterization of the aerosol chemical composition (3.4). The chemical composition corresponding to each air mass has been updated according to the new classification which leads to a change in the figures and tables in section (3.3). This restructuring facilitates its comparison with the other categories and also avoids repetition. The new structure is now:

3.1 Variation of PM10 mass

3.2 Air mass origins

3.3 Characterization of aerosol chemical composition for the complete measurement period

3.4 Inter-relationship between aerosol components

3.5 Day and night-time variation

3.6 Differences in chemical composition between dust and non-dust events

R2-C3: Furthermore, I suggest to make the same type of plots (bar graphs or pie charts) for all these classifications. It makes comparisons between different separation criteria much easier.

R2-A3: We thank the reviewer for the suggestion. The same type of plot, i.e. bar graphs has now been adopted for all the comparisons.

R2-C4: Please give more details on trajectory treatment. Line 456/457 says “The air mass origins were classified into four major categories, as showed in Fig.5.”. But how exactly was that done?

R2-A4: The trajectory analysis was done by grouping samples with similar 12 h trajectories into a cluster and attributing them to a given air mass. If 60% of the hourly trajectories were similar, the sample was allocated to a given air mass category. If they were below this threshold they were considered as mixed and not considered in the classification. In the revised manuscript, corresponding lines have been added on lines 278 to 282 which now read:

“To group the back trajectories into distinct transport patterns, a manual classification approach was used. This method consists of grouping 12 trajectories with the time interval between adjacent nodes of 1 h and calculated for 96 h, and attributing them to a specific air mass category. The assignment of the trajectories was based on their crossing over given latitude-longitude grids attributed to given geographical sectors. To assign a sample to a specific air mass category, 60% of the trajectories must have a similar profile.”

R2-C5: Did you check whether a trajectory crossed a certain latitude-longitude range?

R2-A5: Yes, the trajectories are grouped according to their crossing over given grids, which consist of different longitudes and latitudes. These longitudes and latitudes were attributed to geographical sectors for the better identification of the air mass trajectory. The air masses were then classified considering their geographical origin and four major sectors as follow:

NW sector: Air mass coming from the coast of Europe and crossing the North of Morocco.

W sector: Air mass coming from North Atlantic.

NE sector: Air mass coming from the Mediterranean.

SW sector: Air coming from Saharan dust located at the south-west

R2-C6: How many points were used to assign a trajectory to a certain category?

R2-A6: Each sample contained 12 hourly 96 h back trajectories with a 1h time interval between adjacent nodes. When 60% of the trajectories had a similar profile, they were assigned to a given category. Scenarios representing mixed cases were excluded in the classification as explained above.

Two corresponding sentences have been added on lines 280-282, which now read:

“The assignment of the trajectories was based on their crossing over given latitude-longitude grids attributed to given geographical sectors. To assign a sample to a specific air mass category, 60% of the trajectories must have a similar profile.”

R2-C7: Did you use a clustering algorithm?

R2-A7: We did not apply a clustering algorithm; we did a visual classification based on the frequency of trajectories with similar profiles. However, the obtained results were compared with those of a cluster analysis approach according to Cui et al. (2021) using the HYSPLIT algorithm (Rolph et al. 2017). The results of the air mass categories of the cluster analysis were identical to those obtained with the above approach but differed by about 8% in terms of the frequency associated with the categories above. The results of the comparison have been presented as Supplementary information as Figure S1.

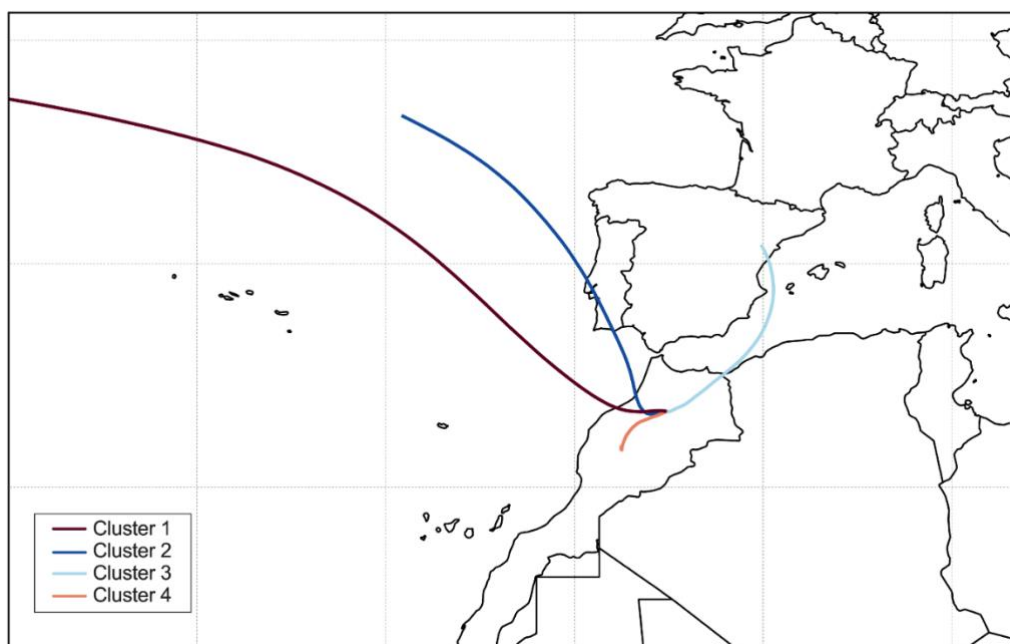


Figure S1. Cluster analysis of back trajectories arriving at AM5 site from August to December 2017 classified into 4 trajectory clusters

R2-C8: Did you consider the vertical motion? It makes a big difference if a trajectory crosses the desert at 2000 m or at 200 m altitude.

R2-A8: The vertical motion was taken into consideration during the backward trajectory calculations and the classification process. The trajectories have been calculated for three different heights (100 m, 500 m, 1000 m) above ground level through the HYSPLIT model. The vertical transport was modeled using the isobaric option of HYSPLIT.

R2-C9: What exactly is shown in Figure 5?

R2-A9: Figure 5 presents 96-hour HYSPLIT backward trajectories shown separately for typical samples that represent an air mass category. The back trajectories were imported as GIS files and plotted using the QGIS software program. The dates for each sample as well as their PM₁₀ mass has been added in the caption of the Figure. The Figure is now updated to include a typical background condition air mass. The new Figure and caption are presented below.

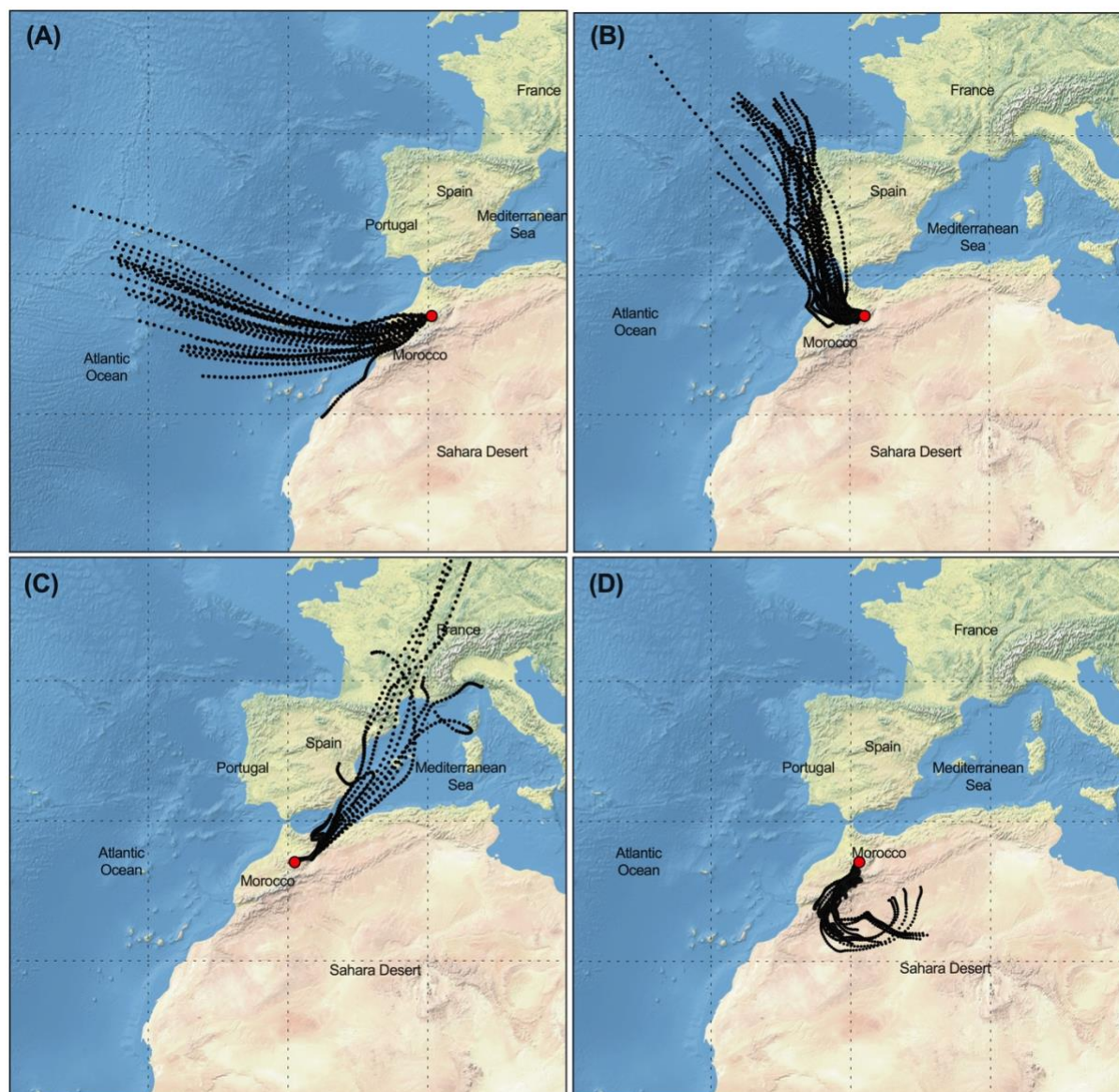


Figure 4. Typical 96h air mass back trajectory performed for AM5 during routine samples periods; aerosol type and PM₁₀ mass concentration are given in parentheses: (a) 18 December 2017: air mass from the North Atlantic Ocean considered to be representative of background conditions (Background, $m=10.9 \mu\text{g m}^{-3}$); (b) 10 October 2017: air mass from Europe crossing coastline of North Morocco (Atlantic Coast Europe, $m=44.1 \mu\text{g m}^{-3}$); (c) 2 November 2017: slightly polluted air mass from North East crossing Mediterranean Sea Morocco (Mediterranean Coast Europe, $m=26.4 \mu\text{g m}^{-3}$); (d) 13 August 2017: dust loaded air mass coming from Sahara desert (Saharan Dust, $m=94.1 \mu\text{g m}^{-3}$).

The paragraph describing the results of updated air mass classification in section air mass origins (3.2) has been modified. The corresponding sentences have been modified in lines 347-357 and now read as follows:

“The calculation of back trajectories using the HYSPLIT model allowed the identification of several remote sources of PM10 at the station. Four main air masses categories were identified as shown in Fig. 4. i) Air masses that spent the last 96h over the Atlantic Ocean at high-altitude (1000 m.asl), representative of typical background air mass (BAM) conditions, which influenced about 5.3% of all samples; ii) Air masses originating from the Atlantic and crossing over the Coast of Europe (ACE), especially Spain and over Moroccan industrial cities located at the North Atlantic coast, influencing about accounts 26.8% of all samples; iii) Air masses from Europe crossing over the Mediterranean Coast and Europe (MCE) as well as over North Moroccan cities, as shown in Fig. 4c and influencing about 37.4% of all samples and iv) Air masses originating from Southern and/or Eastern Sahara crossing the desert (SD), at different altitudes before arriving at the AM5 and influencing about 22.6% of all samples. The remaining back trajectories represent mixing scenarios including 7.9% of all samples that could not be assigned to the four major classes mentioned above.”

R2-C10: How many trajectories of sample times are not shown here?

R2-A10: Some of the samples which represent 8% didn't match the criterion explained above and were representative of the mixed scenario and were, therefore, excluded (n=15). An example is shown below:

A corresponding line has been added on the manuscript on lines 282-283:

“Samples (n=15 samples) with trajectories from mixed origins (e.g., marine air mass over Europe and the desert) were excluded from the classification of the air masses.”

R2-C11: The caption says “PM10 mass concentration are given in parentheses” but only a percentage value is given.

R2-A11: The date and the mass concentration of each distinctive sample have been added to the figure caption as presented above.

R2-C12: Did you check how the local orography is represented in the model? 2000 m starting point may be too high if the model landscape smoothes the actual mountain range down to lower altitudes. HYSPLIT offers the option "above ground level", so initializing the trajectories with "10 m above ground level" might be a good sensitivity test.

R2-A12: We thank the reviewer for pointing out the choice of arrival altitudes for the back trajectory calculation, which is an important step. There was an error in the manuscript, the sentence referred to 2000m above sea level and not ground level. However, as advised, a sensibility test was performed using trajectory calculations at 2000 m above sea level and 10 m, 100m, and 1000m above ground level as references. The trajectories at 1000 m above ground level were found stable and consistent with the trajectories at 2000 m above sea level since the background level height (terrain height) of the grid cell used by HYSPLIT and the GDAS 1 files was 1000 m in this location. The Figure below presents the results of the comparison between 2000m a.s.l and 1000 m a.g.l. The comparison shows similar trajectories. It proves that the sensitivity of the land level is more relevant. Therefore, as suggested by the reviewer, we have recalculated the trajectories using the ground level with an altitude of 1000 m above ground level as a reference as shown in Fig.1 of the supplement. A corresponding line has been added on the manuscript on lines 275-276:

"Due to the resolution of the input data, the exact altitude of the mountain is not properly represented and according to the HYSPLIT model at the AM5 site, the terrain height is at 1000 m only. Therefore, trajectories were calculated every hour for the altitude of 1000 m above model ground."

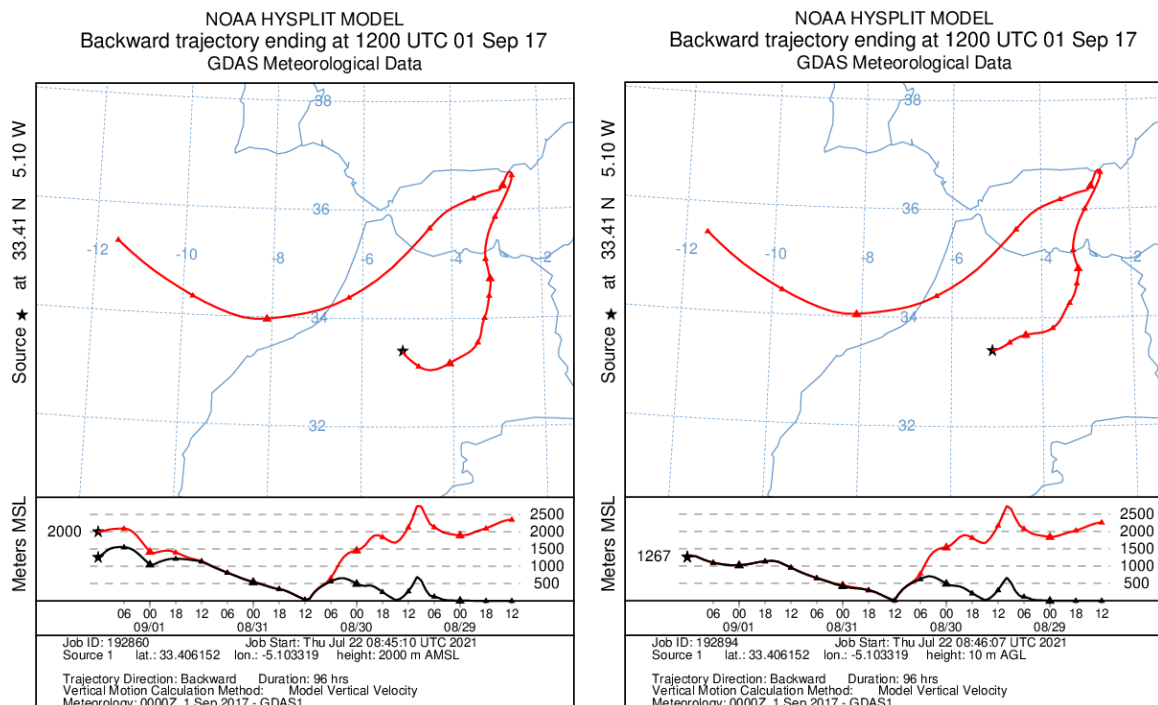


Figure S2. Back trajectory calculated at 1267 m above ground level and 2000 m above sea level.

R2-C13: The definition of the background conditions (“mass concentration lower than 20 $\mu\text{g}/\text{m}^3$ and low wind speeds less than 4 m/s.”) is not clear to me and seems artificial.

R2-A13: This issue was also risen by R1 (comment R1-C4). The choice of the background definition was motivated by different studies such as Puxbaum et al., 2004; Vardoulakis and Kassomenos, 2008; Karaca et al., 2009; Harrison et al., 2004; Escudero et al., 2006 that suggests that the reference could be at 20 $\mu\text{g m}^{-3}$. However, as recommended by R1, the lowest fifth (5th) percentile of PM_{10} mass concentrations has now been considered as the baseline threshold. This can be easily seen in the new PM_{10} variation figure (Fig. 3A). Based on these new criteria, the $\text{PM}_{10} < 12 \mu\text{g}/\text{m}^3$ was considered as background. The number of samples that met these conditions was 10 and the mean concentration was about 10.9 $\mu\text{g m}^{-3}$.

A corresponding text has been added on the manuscript on lines 318-329:

“To establish a reference baseline and evaluate the background conditions at the site, the lower 5th percentile of the PM_{10} concentrations was found to be representative of remote background aerosol conditions. The PM_{10} frequency and probability density function as shown in Fig. S3 confirmed this observation. The samples within this PM concentration range were had similar air mass trajectories and typical meteorological conditions with low wind speeds $< 3 \text{ m s}^{-1}$. The air masses typically traveled in the free troposphere at about 1000 m above sea level, crossing the North-Atlantic Ocean before arriving at the site within the past 96 h. These conditions were, however, not free from local and regional pollution from point sources such as dust resuspension from the cars assessing the site.

Consequently, the average background PM_{10} mass concentration at the Middle-Atlas was 10.9 $\mu\text{g m}^{-3}$, which was found to be stable and representative of periods of little external influence. In comparison, Benchrif et al. (2018) reported background PM_{10} values for Northern Morocco with an average of 12.2 $\mu\text{g m}^{-3}$, which is very similar to the concentrations determined in this study, 10.9 $\mu\text{g m}^{-3}$.”

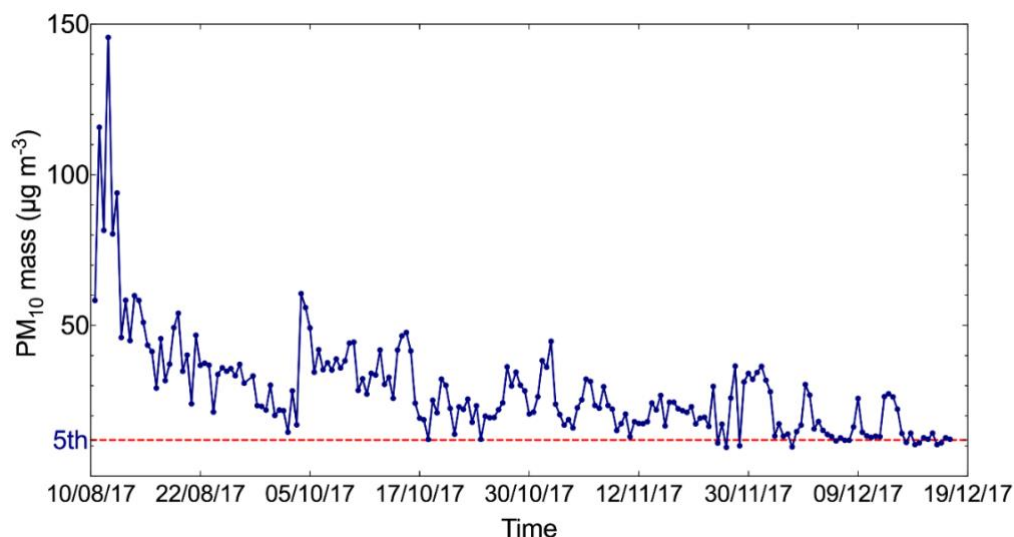


Figure 3. (A) Time series of daily PM₁₀ mass.

R2-C14: More data analysis is required for such a classification. For example, create a PDF (probability density function) of mass concentrations and wind speeds to show that the chosen thresholds are reasonable.

R2-A14: We thank the reviewer for this suggestion. Accordingly and also a reply to R1-C2 the frequency and the probability density function (PDF) of mass concentrations and wind speed were calculated for background samples. The thresholds chosen are in line with the results obtained from statistical calculations, as highlighted with the blue bars in the frequency and probability density function Figures below.

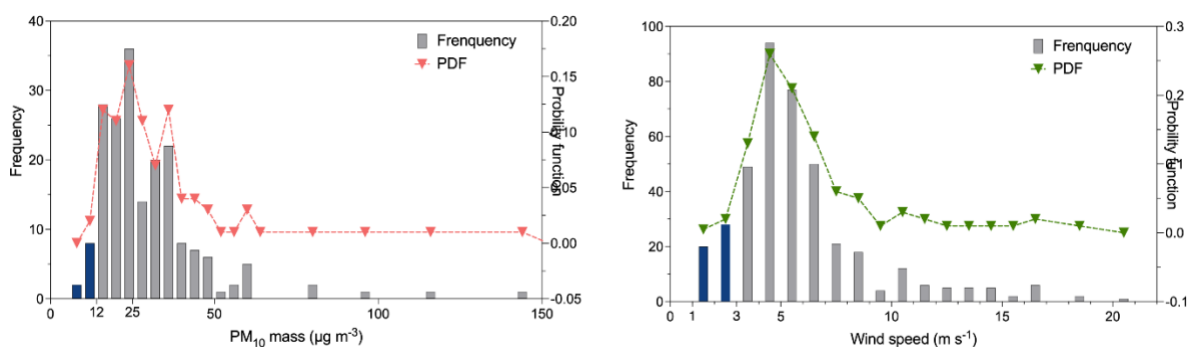


Figure. S3 PM₁₀ mass and wind speed probability density functions during the sampling period.

We have chosen to include these Figures into the SI. A corresponding sentence has been added to the manuscript on line 320:

“The PM₁₀ frequency and probability density function as shown in Fig. S3 confirmed this observation.”

R2-C15: Trajectory information may also be used (see comments above) so check whether the air masses touched the boundary layer or travelled only in the free troposphere.

R2-A15: Trajectory information was used to select the background samples. The samples were of air masses that traveled in the free troposphere at altitudes 1000 m above sea level coming from North-Atlantic Ocean within the past 96 h before arriving at the site. This aspect has been further highlighted in the revised version under section 2.5, lines 322-323:

“The air masses typically traveled in the free troposphere at about 1000 m above sea level, crossing the North-Atlantic Ocean before arriving at the site within the past 96 h.”

R2-C16: A classification based on solid, statistical relevant criteria is needed for this section.

R2-A16: The definition of the background and the selection criteria have been reviewed and are given as follows:

- Samples that lie within the lower 5th percentile of PM₁₀ mass concentrations
- Probability density function (PM₁₀) indicating a range of the lower 5th percentile
- The Wind speeds lower than 3 m s⁻¹
- Samples were typical of air masses coming from the North-Atlantic Ocean crossing free troposphere at altitudes above 1000 m during transport

Further comments

R2-C17: Section “3.1.2 comparison with other stations” and (Table 3): I miss Jungfraujoch and other GAW stations. There is a data base of the GAW stations: <https://gawsis.meteoswiss.ch/GAWSIS/#/>

R2-A17: Urban stations especially in India or China have been removed from the table and replaced by remote high-altitude stations and urban measurements made in Morocco. The station Jungfraujoch and other GAW stations such as Mt. Everest, Mt. Cimone, and puy de Dôme were added to Table 3 to make the comparison more relevant. Other data from urban sites located in Morocco such as Marrakech, Meknes, and Kenitra have also been added. Therefore, Table 3 has been updated and the discussion of the comparison with other sites in section 3.1 on the manuscript has been rewritten and now read in lines 231-345:

“The mean concentration recorded at AM5 from this study ($29.2 \pm 17.3 \mu\text{g m}^{-3}$) agreed well with the PM₁₀ concentration of other remote high-altitude sites, such as Darjeeling in Northeastern Himalayas ($29 \mu\text{g m}^{-3}$; Chatterjee et al. 2010), Lhasa in Tibet ($37 \mu\text{g m}^{-3}$; Wang et al., 2015), and Mahabaleshwar in India ($37 \mu\text{g m}^{-3}$; Leena et al., 2017) as presented in Table 3. Other high-altitude stations, such as Izaña, in Canary Islands ($46 \mu\text{g m}^{-3}$) showed much higher PM₁₀, most likely due to the exposure to strong Saharan dust events (García et al., 2017). In contrast, the PM₁₀ concentrations at AM5 were considerably higher than the PM₁₀ levels recorded in European and Asian high-altitude sites. For example, the average PM₁₀ mean value recorded in this study was about twice that of Mount Cimone, Italy ($16 \mu\text{g m}^{-3}$; Marenco et al., 2006) and factor 6 greater than the PM₁₀ in

Everest Mountain (Decesari et al., 2010) and in Puy de Dôme, France ($6 \mu\text{g m}^{-3}$; Bourcier et al. 2012), and was approximately 10 times greater than the average level in Jungfrauoch ($3 \mu\text{g m}^{-3}$; Cozic et al., 2008). Other Moroccan sites, such as Marrakech, Meknes, and Agadir, which are exposed to strong urban emissions, usually show PM_{10} concentrations between 50 and $110 \mu\text{g m}^{-3}$, which is much higher than the concentration found at AM5 in this study (Inchaouh, 2017; Tahri et al., 2013, 2017). These results highlight a better air quality at AM5 in comparison to many sites and indicate that the station can serve as a good remote reference station for defining background concentrations in Morocco and possibly the whole of North Africa.”

Table 3. Average mass concentration of PM_{10} from other high-altitude sites and urban sites in Morocco reported in the literature according to altitude.

N°	Site	Site type	Sampling Period	Altitude (m)	PM_{10} ($\mu\text{g m}^{-3}$)	References
1	Mt. Everest, Nepal	High altitude	Feb 2006-May 2008	5079	6	Decesari et al., 2010
2	Lhasa, Tibet	High altitude	Jan-Feb 2006	3663	37	Wang et al., 2015
3	Jungfrauoch, Switzerland	High altitude	Feb-Mar 2005	3580	3	Cozic et al. 2008
4	Izaña, Canary Islands	High altitude	Feb 2008-Aug 2013	2400	46	García et al., 2017
5	Mount Cimone, Italy	High altitude	Jun-Aug 2004	2165	16	Marenco et al. 2006
6	Atlas (AM5), Morocco	High altitude	Aug-Dec 2017	2100	29	Present study
7	Puy de Dome, France	High altitude	Apr 2006-Apr 2007	1465	6	Bourcier et al. 2012
8	Mahabaleswar, India	High altitude	Jun 2012-May 2013	1348	37	Leena et al., 2017
9	Djarjeeling, India	High altitude	Jan-Dec 2005	2194	29	Chatterjee et al. 2010
10	Marrakech, Morocco	Urban	2009-2012	465	55	Inchaouh et al., 2017
11	Meknes, Morocco	Urban	Mar 2007-Apr 2008	546	75	Tahri et al., 2012
12	Tetouan, Morocco	Urban	May 2011-Apr 2012	105	31	Benchrif et al., 2018
13	Kenitra, Morocco	Urban	Feb 2007-Feb 2008	26	110	Tahri et al., 2017

The former Table 4 contains the chemical composition only during background conditions and has now been modified. Now Table 5 gives the chemical composition for the entire sampling period compared to other high elevation sites as shown in the following.

Table 5. Concentrations of main aerosol chemical species in PM₁₀ (ng m⁻³) at AM5 compared to other high altitude mountain stations. Data are reported in the format average (mean ± standard deviation) and NA: not available. Notice that the concentrations of PM₁₀ mass are given in µg m⁻³. ^a Present study; ^b Bourcier et al. 2012; ^c Chatterjee et al. 2010; ^d Marenco et al. 2008; ^e Decesari et al., 2010.

Elements	Mt. Atlas, Morocco ^a	Mt. Puy de Dome, France ^b	Mt. Himalaya, India ^c	Mt. Cimone, Italy ^d	Mt. Everest, Nepal ^e
Altitude (m a.s.l)	2100 m	1465 m	2194 m	2165 m	5079 m
Samples	190	NA	111	57	99
Period	Aug-Dec 2017	Apr 2006-Apr 2007	Jan-Dec 2005	Jun-Aug 2004	Apr 2006 - May 2008
Mass load	29.1 ± 17.3	5.6 ± 4.6	29.5 ± 20.8	16.1 ± 9.8	5.6 ± 4.6
OC	1069 ± 818	NA	NA	NA	800 ± 637
EC	247 ± 134	NA	NA	NA	115 ± 132
Na ⁺	186 ± 231	NA	2200 ± 2000	NA	24.2 ± 22.5
K ⁺	42 ± 35	NA	310 ± 210	NA	34 ± 32
Ca ²⁺	649 ± 579	15.5 ± 10.2	130 ± 10	360 ± 550	138 ± 90
Mg ²⁺	60 ± 50	NA	120 ± 60	NA	19.3 ± 7.2
Cl ⁻	80 ± 133	NA	2350 ± 1500	82 ± 98	22 ± 46
NH ₄ ⁺	298 ± 220	297 ± 276	50 ± 40	1400 ± 800	175 ± 183
NO ₃ ⁻	859 ± 687	510 ± 980	950 ± 200	840 ± 770	170 ± 223
SO ₄ ²⁻	941 ± 848	1380 ± 1160	3500 ± 2100	3500 ± 2000	394 ± 329
Al	443 ± 830	NA	NA	300 ± 460	740
Fe	486 ± 728	NA	NA	260 ± 440	NA
Ti	37 ± 45	NA	NA	30 ± 50	NA
V	3.5 ± 12.2	NA	NA	3.1 ± 1.5	NA
K	174 ± 156	NA	NA	160 ± 210	NA
Cr	4.3 ± 5.2	NA	NA	NA	NA
Ni	2.4 ± 3.1	NA	NA	1.4 ± 0.5	NA
Cu	1.2 ± 3.1	NA	NA	2.9 ± 3.1	NA
Zn	8.6 ± 6.2	NA	NA	9.9 ± 6.6	NA
Pb	4.8 ± 4.5	NA	NA	3.9 ± 2.4	NA
Mn	12.4 ± 39.3	NA	NA	6.2 ± 7.0	NA

The comparison of the chemical composition at AM5 has been added with other high altitude sites in section 3.3. The corresponding sentences have been added as follows:

In lines 395-398: “For instance, the high-altitude site in Mt. Cimone, Italy recorded several days with African dust transport which influenced the chemical composition (Marenco et al., 2006). However, the Saharan dust concentration at AM5 (17.7 µg m⁻³) is approximately 4 times higher than at Mt. Cimone (4 µg m⁻³).”

In lines 398-400: “Nevertheless, the average concentrations of elements such as Al, Fe, Ti, and Mn, are comparable with the values reported in Mt. Cimone, Italy (Marenco et al., 2006), Table 5. However, the calcium, concentration at the AM5 (0.65 ± 0.58 µg m⁻³), was 2 times higher than the concentration recorded in Mt. Cimone.”

In lines 401-402: “Furthermore, the calcium concentration was 5 times higher than the concentration recorded at other high-altitude station such as Mt. Himalaya and Mt. Everest (Chatterjee et al. 2010; d; Decesari et al., 2010).”

In lines 404-405: “Some studies have reported the high content of calcite in the soils of Northern Morocco $1.07 \mu\text{g m}^{-3}$ which confirms the predominance of calcium-rich in the Atlas regions (Desboeufs and Cautenet, 2005; Kandler et al., 2009; Benchrif et al., 2018).”

In lines 432-435: “The study of Decesari et al. 2010 reported similar concentrations of OC ($0.8 \pm 0. \mu\text{g m}^{-3}$), and lower EC ($0.11 \pm 0.13 \mu\text{g m}^{-3}$) concentrations in PM10 at the Himalayan high-altitude station in Nepal. Furthermore, Sharma et al., 2020 reported higher OC ($5.4 \pm 2.0 \mu\text{g m}^{-3}$) and EC ($2.2 \pm 2.0 \mu\text{g m}^{-3}$) at the high-altitude site of Darjeeling, India most likely due to the higher influence of anthropogenic activities at the site.”

In lines 346-449: “The OC/EC ratio observed at AM5 for BAM was similar to those found in local samples in Northern Morocco with an average of 1.9 (Benchrif et al. 2018). Moreover, the OC/EC ratio shows a slight difference with those observed in Mt. Everest (Decesari et al., 2010) whose ratios varied from 5 to 9.”

In lines 476-481: “The comparison of sodium and chloride concentrations with other high-altitude studies is shown in table 5. The concentrations of Na^+ ($1.8 \pm 2.31 \mu\text{g m}^{-3}$) and Cl^- ($0.80 \pm 1.33 \mu\text{g m}^{-3}$) are several times lower than those at Darjeeling in India which has a concentration of Na^+ and Cl^- , of $2.2 \pm 2.0 \mu\text{g m}^{-3}$ and $2.3 \pm 1.5 \mu\text{g m}^{-3}$, respectively. On the other hand, the concentration of Na^+ and Cl^- were 4 to 8 times higher than the values reported at Mt. Everest station located at an altitude of 5079 m asl. In addition, the concentration of chloride was in good agreement with those observed in Mt. Cimone, Italy, $0.82 \pm 0.98 \mu\text{g m}^{-3}$ ”.

In lines 481-484: “Sea salt concentration observed at the AM5 ($0.45 \mu\text{g m}^{-3}$) was 5 times lower than at Tetouan ($2.46 \mu\text{g m}^{-3}$), a coastal Mediterranean city in northern Morocco, and approximately 20 times lower than Cap Verde Atmospheric Observatory (CVAO) located in the tropical Atlantic Ocean (Benchrif et al. 2018; Fomba et al. 2014).”

In lines 504-508: “Secondary inorganic aerosol over the Atlas Mountains has been compared with the data reported in other high-altitude stations (Table 5). The average concentration of nitrate ($0.8 \pm 0.6 \mu\text{g m}^{-3}$) at AM5 was comparable with those reported in Mt. Himalaya and Mt. Cimone, $0.9 \pm 0.2 \mu\text{g m}^{-3}$ and $0.8 \pm 0.7 \mu\text{g m}^{-3}$, respectively (Chatterjee et al. 2010; Marengo et al., 2006). However, the concentration of NO_3^- were found to be approximately 2 times higher than the value reported in Puy de Dôme (Bourcier et al., 2012), as shown in Table 5”.

In lines 513-516: “Similar concentrations of ammonium at AM5 ($0.3 \pm 0.2 \mu\text{g m}^{-3}$) were found at Puy de Dôme, France ($0.3 \pm 0.2 \mu\text{g m}^{-3}$), whereas the concentration was 5 times lower than those reported in other high-altitude sites such as the Mt. Himalaya (Chatterjee et al., 2010). This indicates that the influence of ammonium remains relatively low despite the proximity of the site to agricultural activities located in the surroundings of Meknes.”

In lines 517-519: “The concentrations of sulfate ($0.9 \pm 0.8 \mu\text{g m}^{-3}$) over AM5 were comparable with those at Puy de Dôme ($1.3 \pm 1.1 \mu\text{g m}^{-3}$), but were almost 4-5 times lower than all the other hilly stations except Mt. Everest (Decesari et al., 2010).”

R2-C18: Figure 6: Background shading type is too coarse, hard to recognize

R2-C18: The background shading type has been modified to improve visibility. Thus, each sample is represented by a distinguishing color symbol for each specific air mass. At the same time, Figure 6, which shows the temporal variation of the organics, has been modified in the same way. The new Figure 5 and Figure 6 are shown below:

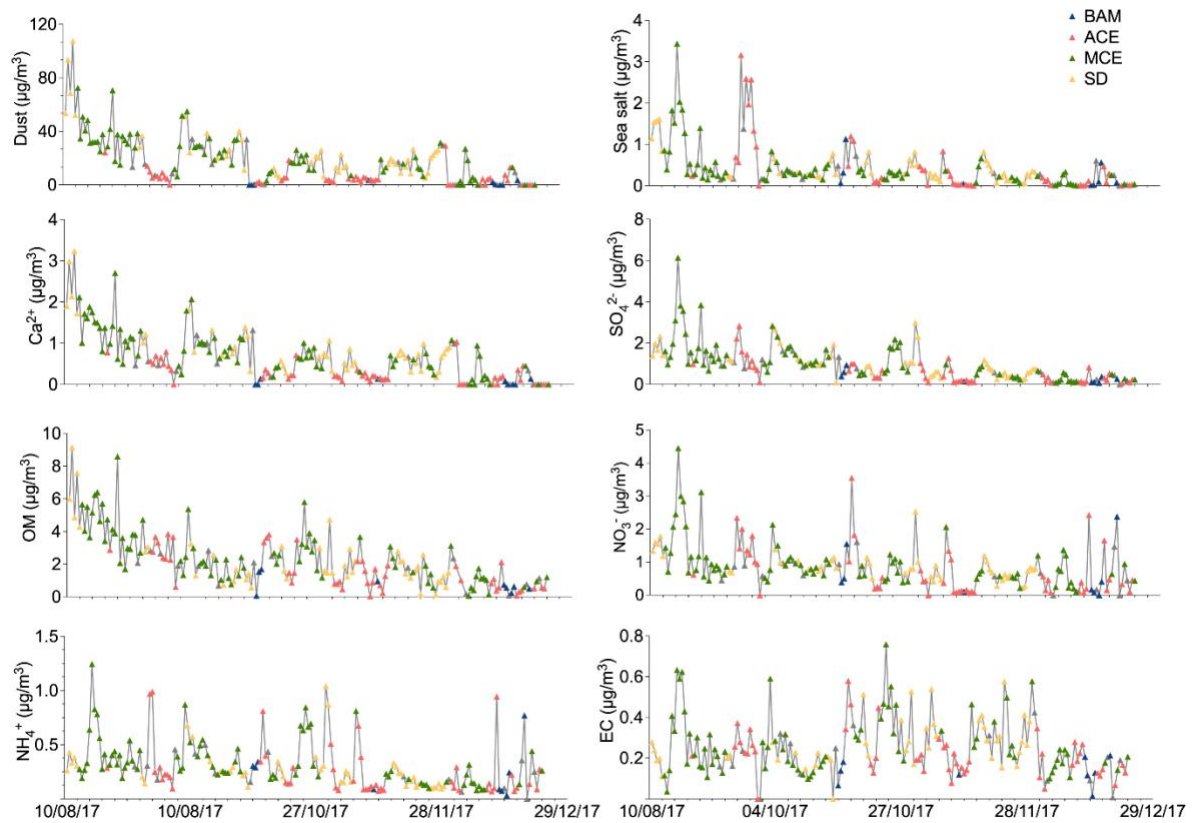


Figure 5. Time series of major aerosol chemical constituents in PM₁₀ filter samples collected from August to December 2017; The color of the symbols displayed for each sample represents a specific air mass origin: Background (blue); ACE (red); MCE (green); SD (yellow).

The description of Figure 6 has been modified in section 3.3 according to the new air mass classification, so the modified paraphrases are listed as follows:

In lines 364-368: "During the 5 months of PM collection at the AM5 site, the average mineral dust concentration was about $17.7 \pm 7.4 \mu\text{g m}^{-3}$ and varied strongly between $0.05 \mu\text{g m}^{-3}$ and $107 \mu\text{g m}^{-3}$. The highest mean concentrations were observed in August ($39 \mu\text{g m}^{-3}$) and the lowest in December ($3.7 \mu\text{g m}^{-3}$). Low concentrations were observed during days with low wind speeds ($< 2 \text{ m s}^{-1}$), low Saharan dust air mass inflow, and after precipitation events, which typically occurred in the fall and winter."

In lines 404-415: "Organic carbon (OC) and elemental carbon (EC) showed strong variation and distinct differences with an average of $1.1 \pm 0.8 \mu\text{g m}^{-3}$ and $0.2 \pm 0.1 \mu\text{g m}^{-3}$, respectively. The OC has both primary and secondary origin, and can be formed from primarily emitted substances through condensation or chemical reactions among them (Sarkar et al., 2019). The OC concentration reached a maximum $4.5 \mu\text{g m}^{-3}$ during summer, whereas the lowest concentration was observed during winter at about $0.03 \mu\text{g m}^{-3}$. The average concentration of OC progressively decreased from summer ($2.1 \pm 0.8 \mu\text{g m}^{-3}$) to winter ($0.3 \pm 0.2 \mu\text{g m}^{-3}$). The abundant contribution of organic matter in summer can be due to high biogenic emissions in the Middle Atlas. A slight increase in OC was also observed during dust events, as shown in Fig. 5, which suggests that the dust deposited at AM5 also contained biogenic material from the surroundings of the Middle-Atlas region."

In lines 464-469: "The Middle Atlas region is influenced by two maritime sources of sea salt, more often from the Atlantic Ocean, and sometimes from the Mediterranean Sea. During the study period, the average concentration of sea salt remains low ($0.45 \pm 0.55 \mu\text{g m}^{-3}$) and contributed only 1.6% of the total PM_{10} concentration. The highest concentrations were recorded during August when sea salt concentrations reached a maximum of $3.4 \mu\text{g m}^{-3}$. The sea salt then decreased gradually, reaching a minimum concentration of $0.06 \mu\text{g m}^{-3}$ during December. The sea salt concentration was high when wind speed exceeded 6 m s^{-1} , indicating that sea salt is strongly dependent on meteorological conditions and air mass sources."

In lines 487-498: "A significant part of PM composition was associated with the formation of secondary inorganic aerosols (SIA), which are mainly composed of sulfate, nitrate, and ammonium. They made up about 7.2% of the PM_{10} mass. The temporal variation during the sampling period of SO_4^{2-} , NO_3^- , and NH_4^+ is presented in Fig. 6, with average concentrations of $0.9 \pm 0.8 \mu\text{g m}^{-3}$, $0.8 \pm 0.6 \mu\text{g m}^{-3}$, and $0.3 \pm 0.2 \mu\text{g m}^{-3}$, respectively. In summer, the concentrations were relatively high during few days in August, with the observation of the highest sulfate, nitrate, and ammonium concentrations of up to $6.1 \mu\text{g m}^{-3}$, $4.4 \mu\text{g m}^{-3}$, and $1.2 \mu\text{g m}^{-3}$, respectively (Fig. 6). This was due to the transport of polluted MCE air masses through the Mediterranean Sea and across cities in the North of Morocco leading to high PM loaded aerosols. On average, the influence of long-range transport during the ACE and MCE air masses for sulfate ($2.8 \mu\text{g m}^{-3}$) and nitrate ($2.3 \mu\text{g m}^{-3}$) were similar. However, the contribution of ammonium ($1.7 \mu\text{g m}^{-3}$) to particulate matter was particularly higher for MCE air mass. Additionally, other peaks were also observed in aerosol concentrations both for SO_4^{2-} and NO_3^- during August. This could be attributed to the long-range transport of dust aerosol from the Saharan desert in Southern Morocco. The subsequent months demonstrate a clear decreasing trend of SIA from high concentrations in summer ($3.8 \mu\text{g m}^{-3}$), to relatively low concentrations during winter ($1.0 \mu\text{g m}^{-3}$)."

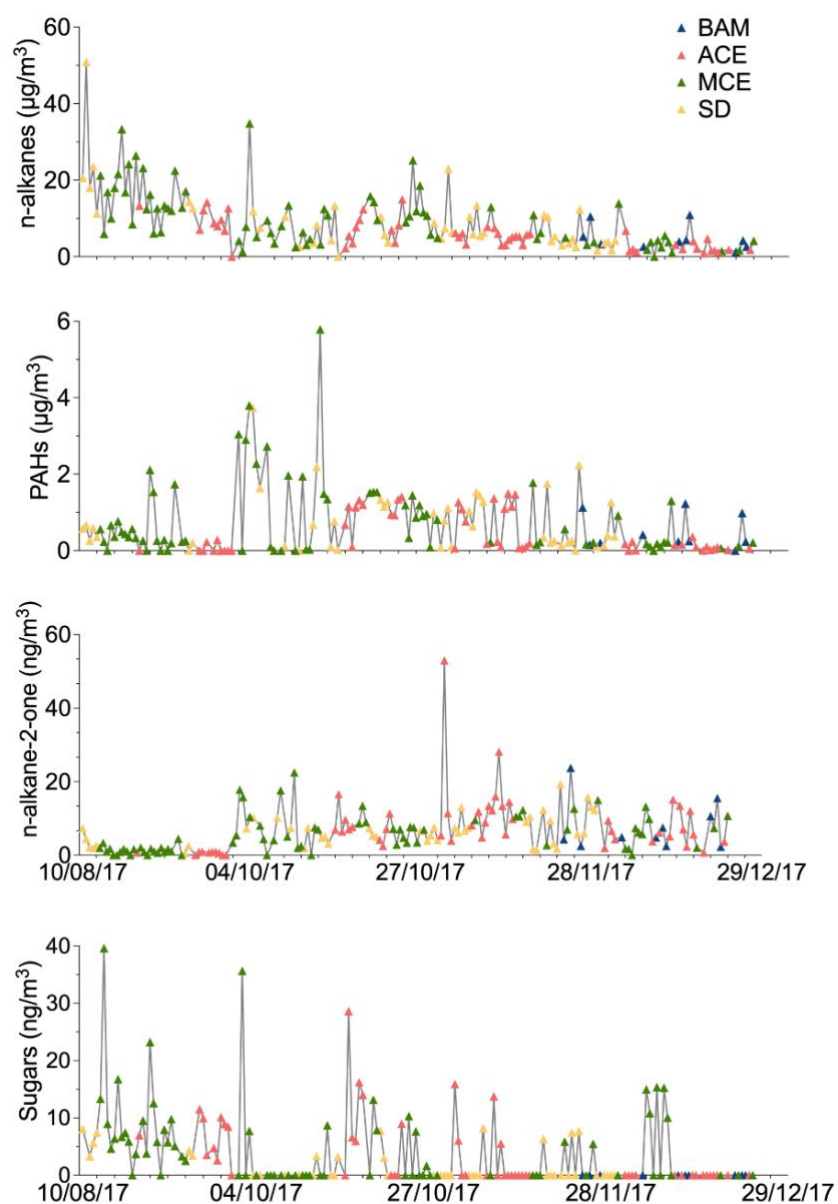


Figure 6. Time series of organic compounds in PM₁₀ filter samples collected from August to December 2017 at AM5; The color of the symbols displayed for each sample represents a specific air mass origin: Background (blue); ACE (red); MCE (green); SD (yellow).

The description of Figure 6 has been modified in organic compounds section (3.3.5) according to the new air mass classification, so the modified paraphrases are listed as follows:

In lines 529-533: "The distinguishing aspect of alkanes is their specific source and their ability to provide information about their origins (Pietrogrande et al., 2010). Individual n-alkanes with C-atom numbers in the range 19-34 were analyzed. Figure 6 shows the temporal variation of the n-alkanes revealing strong variations over the seasons with an average concentration of about $8.4 \pm 7.1 \text{ ng m}^{-3}$. The average concentration decreases from summer ($16.1 \pm 8.9 \text{ ng m}^{-3}$) to winter ($2.6 \pm 2.0 \text{ ng m}^{-3}$)."

In lines 566-572: "In the present study, polycyclic aromatic hydrocarbons (PAHs) with 3 to 7 rings were quantified. The temporal variation of the sum of the 20 identified PAH compounds in the particle is presented in Figure 6. The contribution of PAHs remains much lower than alkanes with an average concentration of $0.7 \pm 0.8 \text{ ng m}^{-3}$ over the whole study period. Contrary to what has been observed for alkanes, the PAH concentrations determined during the autumn months are higher than those during the summer and winter: The highest amount of PAH was detected during October, approximately 5.8 ng m^{-3} due to long-range transport of MCE air masses, as shown in Figure 6. The minimum concentration was observed during winter, of about 0.05 ng m^{-3} ."

In lines 590-598: "In total, 5 n-alkan-2-ones were detected in this study, as shown in Fig. S8. The n-alkan-2-one concentrations increased significantly from summer (1.8 ng m^{-3}) to autumn (9.7 ng m^{-3}), then decreased continuously to winter (6.3 ng m^{-3}), with an average of 6.6 ng m^{-3} for the whole sampling period. The minimum concentration was recorded during the summer of about 0.60 ng m^{-3} . In contrast, the maximum concentration was reached during autumn of about 52 ng m^{-3} due to ACE air mass influence, as shown in Fig. 6. The sum of n-alkane-2-one was between 0.67 to 13.2 ng m^{-3} . The same relative composition of n-alkan-2-one concentrations was observed in both seasons, suggesting that they came from similar sources. However, the levels of n-alkan-2-one were much lower in concentration than those of n-alkanes. The average background concentration of the total n-alkan-2-one was $5.9 \pm 5.5 \text{ ng m}^{-3}$."

R2-C18: Table 5: First-row "mass load NOA": should it read "109"?

R2-C18: Indeed, a typing error was made in Table 5, the mass of NOA was $19 \mu\text{g m}^{-3}$, and the mass of dust was $9.6 \mu\text{g m}^{-3}$. Nevertheless, Table 5, which became Table 4 in the new version of the manuscript, presents the updated chemical composition of the new classification. Thus, the NOA has been combined with the ACE and a new category representing the Background conditions has been included. The chemical composition has been expanded by adding elements that are relevant in the comparison between the different categories. The respective standard deviation for each category was also added. The update of Table 5 is present as follows:

Table 4. Concentrations of main aerosol chemical species in PM₁₀ according to each air mass ($\mu\text{g m}^{-3}$) at AM5; The organic composition is given in ng m^{-3} ; The number of samples is written in parentheses.

Aerosol components	Air mass			
	BAM (n=10)	ACE (n=51)	MCE (n=71)	SD (n=43)
Mass load	10.9 ± 0.9	20.4 ± 6.3	33.8 ± 14.5	37.9 ± 25.3
Dust	5.5 ± 3.5	13.3 ± 5.2	19.9 ± 11.9	29.1 ± 22.6
Sea salt	0.05 ± 0.06	0.3 ± 0.5	0.3 ± 0.4	0.2 ± 0.2
OM	1.0 ± 0.6	1.4 ± 1.1	2.7 ± 1.7	2.3 ± 1.8
EC	0.2 ± 0.1	0.2 ± 0.1	0.2 ± 0.1	0.2 ± 0.1
POC	0.1 ± 0.06	0.2 ± 0.3	0.3 ± 0.3	0.2 ± 0.2
SOC	0.3 ± 0.2	0.4 ± 0.4	1.0 ± 0.8	0.9 ± 0.8
NO ₃ ⁻	0.5 ± 0.6	0.6 ± 0.7	1.0 ± 0.7	0.9 ± 0.4
nss-SO ₄ ²⁻	0.2 ± 0.2	0.5 ± 0.5	1.2 ± 0.9	1.0 ± 0.6
NH ₄ ⁺	0.2 ± 0.2	0.2 ± 0.2	0.3 ± 0.2	0.2 ± 0.1
Ca ₂ ⁺	0.2 ± 0.2	0.2 ± 0.2	0.8 ± 0.5	0.9 ± 0.6
Alkanes	4.9 ± 3.2	5.6 ± 3.7	10.5 ± 7.7	9.2 ± 8.6
PAHs	0.4 ± 0.5	0.4 ± 0.4	0.9 ± 2.1	0.7 ± 0.7
Alkan-2-ones	7.8 ± 6.9	5.9 ± 5.5	5.5 ± 5.0	6.6 ± 4.1
Sugars	-	3.7 ± 6.0	5.2 ± 7.7	1.8 ± 2.9
Oxalate	44 ± 26	73 ± 58	129 ± 58	107 ± 63
pH	5.6 ± 0.2	6.0 ± 0.4	6.5 ± 0.4	6.5 ± 0.4
OC/EC	2.2 ± 1.1	3.3 ± 1.9	6.3 ± 7.5	4.6 ± 4.6
CPI	3.3 ± 0.8	3.5 ± 2.4	3.9 ± 1.9	4.0 ± 3.1

The comparison between the chemical composition with respect to the air masses (Table 4) have been included in the discussion paragraphs in section (3.3). The corresponding sentences have been added as follow:

In lines 383-389: “Mineral dust was found to be more than 7 times higher ($37.9 \pm 25.3 \mu\text{g m}^{-3}$) during dust events (SD), in comparison to remote background conditions (BAM) with an average concentration of $5.5 \pm 3.5 \mu\text{g m}^{-3}$, as observed in Table 4. Other less intense Saharan dust storms occurred during the summer season between the 21st and 24th of August with a similar high dust concentration that was 5 times higher than dust background concentrations. The presence of mineral dust is relatively low but still significant for air masses other than SD, such as during the ACE ($13.3 \pm 5.2 \mu\text{g m}^{-3}$) and MCE ($19.9 \pm 11.9 \mu\text{g m}^{-3}$) air mass influence, as shown in Table 4.”

In lines 444-445: “The highest OC/EC ratio (6.3 ± 7.5) was observed for MCE air masses, while the lowest ratio was recorded for BAM at about 2.3 ± 1.1 , as shown in Table 4.”

In lines 462-463: “However, no significant difference was noticed in sea salt concentrations found in the ACE ($0.5 \pm 0.7 \mu\text{g m}^{-3}$) and MCE samples ($0.5 \pm 0.5 \mu\text{g m}^{-3}$), as shown in Table 4.”

In lines 494-496: “On average, the influence of long-range transport during the ACE and MCE air masses for sulfate ($2.8 \mu\text{g m}^{-3}$) and nitrate ($2.3 \mu\text{g m}^{-3}$) were similar. However, the contribution of ammonium ($1.7 \mu\text{g m}^{-3}$) to particulate matter was particularly higher for MCE air mass.”

In lines 550-552: “Table 4 presents the CPI values calculated according to each air mass. The average CPI value was 3.8 ± 2.4 and ranged from 0.7 to 18.6. However, high CPI ($\gg 1$) was observed for all air masses, which indicates that the alkanes originated from plants waxes, as presented in Table 4 (Kavouras, 2002).”

In lines 570-575: “The highest amount of PAH was detected during October, approximately 5.7 ng m^{-3} due to long-range transport of MCE air masses, as shown in Figure 6. The minimum concentration was observed during winter, of about 0.05 ng m^{-3} . The average background concentration of PAHs was $0.4 \pm 0.5 \mu\text{g m}^{-3}$, which was low in comparison to other organic compounds likely because of high evaporation on warm days (Cincinelli et al., 2007). During MCE air mass, the PAH concentrations increased by 52% compared to the BAM concentration, as shown in Table 4.”

In lines 630-641: “The average sugar concentrations during these air mass influences were ACE ($3.7 \pm 6.0 \text{ ng m}^{-3}$) and MCE ($5.2 \pm 7.7 \text{ ng m}^{-3}$), as listed in Table 4. In contrast, sugar compounds were relatively low in SD ($1.8 \pm 2.9 \text{ ng m}^{-3}$) air masses and were not found in the background PM_{10} conditions. Levoglucosan which is considered as a good tracer of biomass burning emissions in aerosol particulate matter, was particularly higher for ACE (2.0 ng m^{-3}) and MCE (1.6 ng m^{-3}) air mass influence, as displayed in Fig. S8. (Bauer et al., 2008). Arabitol shows a similar concentration for MCE and ACE with a mean of 1.0 ng m^{-3} suggesting that particles were loaded with primary biological aerosols such as pollen, fungal spores, vegetative debris, viruses, and bacteria from the marine coast (Fu et al., 2012). Glucose remained relatively high during MCE air mass influence in comparison to other air masses influence. During SD air mass influence, the concentration of arabitol was extremely low with a concentration less than 0.08 ng m^{-3} . However, glucose showed a higher concentration of about 0.7 ng m^{-3} but remains 3 times lower than MCE concentrations. This indicates that the sugars were most likely originated from marine air masses.”

Figure 7 has been updated according to the new air mass classification. The category of Background Air Mass has been added as follow:

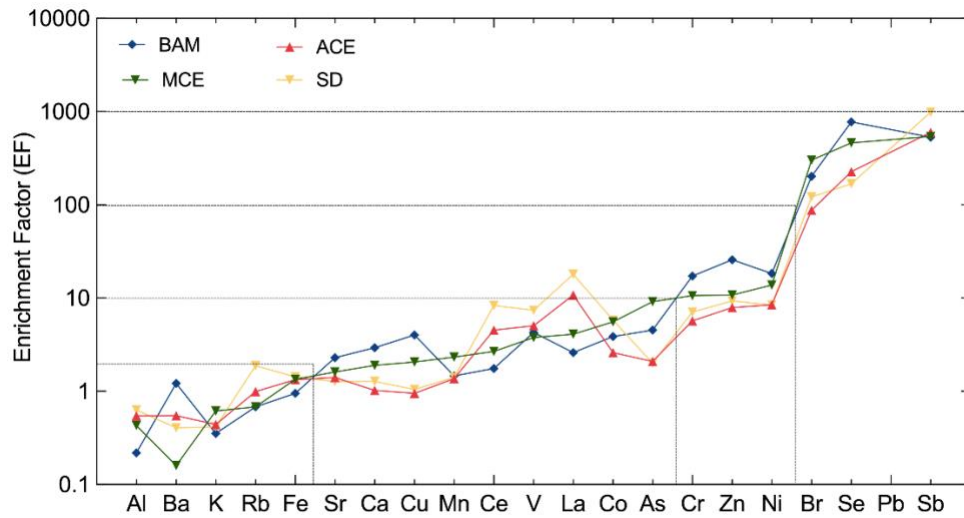


Figure 7. Crustal enrichment factors (EF) of aerosol PM₁₀ evaluated for the different trace metal elements at AM5; The averaged values are plotted according to their respective air mass origins.

The correlation plot displayed in Figure 8 have been updated according to the new air mass classification as follow:

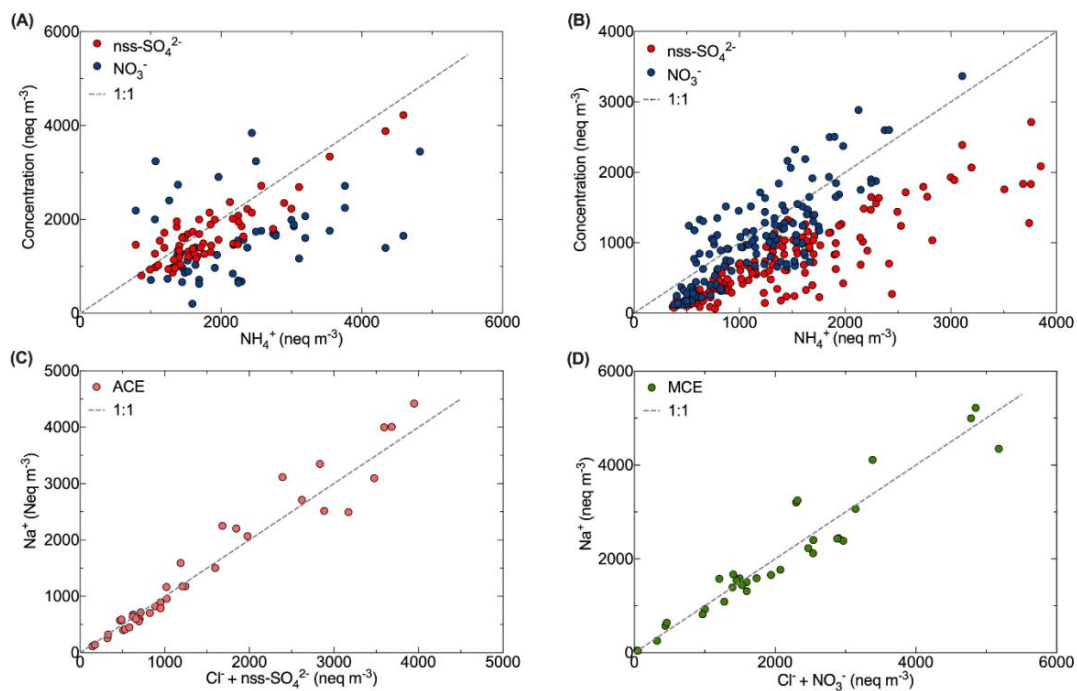


Figure 8. Scatter plot of (A) NH₄⁺ with NO₃⁻ and nss-SO₄²⁻ during summer; (B) NH₄⁺ with NO₃⁻ and nss-SO₄²⁻ during autumn-winter; (C) Na⁺ and Cl⁻ + SO₄²⁻ during ACE air mass; (D) Na⁺ and Cl⁻ + NO₃⁻ during MCE air mass at the AM5 site.

The inter-relationship between aerosol components section (3.4) has been restructured by adding subheadings as follow:

3.4.1 Nitrate and nss-sulfate

3.4.2 Ammonium nitrate and ammonium sulfate

3.4.3 Sodium and chlorine

Therefore, the discussion paragraphs of different correlations have been reformulated as follow:

In lines 708-721: “The correlation between NO_3^- and nss-SO_4^{2-} ($r^2=0.76$) indicates their possible common origin. The correlation was more pronounced for MCE air masses ($r^2=0.80$) in contrast to ACE ($r^2=0.43$) air masses, suggesting an enhanced transport of secondary anthropogenic aerosol from the Mediterranean coast (Liu et al., 2017) to the AM5 site. The nss-sulfate concentrations were slightly correlating with Vanadium which is associated with the emissions of oil combustion, ship emissions as well as iron and steel industrial emissions (Pandolfi et al., 2011). A strong correlation of NO_3^- and nss-SO_4^{2-} was observed with oxalate ($\text{C}_2\text{H}_4^{2-}$), which could indicate that they have a common source and that they can originate from biomass burning and secondary transformations. Nss-SO_4^{2-} also originated from crustal sources especially as elevated concentrations were observed during dust events. This assertion was supported by a good correlation of nss-SO_4^{2-} with nss-Ca^{2+} (Fig. S7), indicating the likely presence of calcite particles of crustal origin. A similar observation was reported by Okada and Kai, (2004), who observed that Desert dust was associated with sulfur compounds and organic matter from surrounding agricultural areas. Indeed, the particles with high sulfate content were accompanied by Ca and were assigned as gypsum particles, also suggesting that the sulfur in these particles originated from a sedimentary source (Falkovich et al., 2001).”

In lines 728-741: “The analysis of the correlation matrices between nss-SO_4^{2-} and NO_3^- with ammonium (NH_4^+) was applied to better understand the inter-relationship between the secondary inorganic species. A correlation between nss-SO_4^{2-} and NH_4^+ ($r^2= 0.90$) supported the hypothesis of dominant ammonium sulfate particles $(\text{NH}_4)_2\text{SO}_4$ in the summer especially when air masses were coming from ACE, as shown in Fig. 8. During this period, a strong correlation was found between sulfate and solar radiation which suggests that nss-SO_4^{2-} was produced via photochemical reaction (Baker and Scheff, 2007). Nevertheless, the transport of nss-SO_4^{2-} from the Atlantic coast also contributes to the formation of ammonium sulfate. However, the trend is more towards ammonium nitrate (NH_4NO_3) in winter, given that the main correlation of NH_4^+ with NO_3^- ($r^2= 0.95$) mainly present in MCE air masses. Nitrate shows a strong dependency on the temperature at AM5, most likely due to the stability of ammonium nitrate in the atmosphere at low temperatures (Squizzato et al., 2013). The predominance of nitrates over sulfates during winter, where nitrates and ammonium remain high, is probably due to the influence of temperature that prevents the dissociation of ammonium nitrate particles (Ricciardelli et al., 2017). Moreover, a similar pattern of NO_3^- and NH_4^+ as observed by Querol et al., 2004 in the Mediterranean coast with a summer minimum and suggested that it could be due to the low thermal stability of the nitrate in the hot season.”

In lines 738-750: “The evolution of the sea salt constituents and their relationship with the most important aerosol acidic species such as NO_3^- and SO_4^{2-} was investigated according to their air mass origins (Fig. 8). A correlation

between sodium and chlorine was observed ($r^2=0.76$), as shown in Fig. 8. The scatter plot of molar equivalent concentrations of Na^+ and Cl^- shows a strong correlation specifically for ACE and SD air masses. However, the data points are below the seawater reference line and only approach this line when the Cl^- concentration is combined with NO_3^- and nss-SO_4^{2-} . This indicates that chloride was depleted in the sea salt particles due to the displacement of chloride by sulfate from sulfuric acid when air masses were coming from MCE and ACE, especially as photochemical processes favor sulfate formation during summer. The same scenario has been observed for NO_3^- with a considerable difference during the winter. Indeed, the correlation between sodium and the sum of chloride and nitrate shows the chloride depletion and indicates that the Mediterranean Sea air mass was loaded with aged sea salt. Similar results were observed in the North of Morocco where the mass fraction of nitrate was higher in the coarse fraction which indeed corresponds to aged sea salt (Benchrif et al. 2018). No correlation between Na^+ and Cl^- was observed in the BAM conditions.”

R2-C19: Data availability: Please make the data publicly available through a database or repository. The data set should be easy to handle (a simple table with date, time, concentration of compounds) for everybody.

R2-C19: The data are available upon request and will be uploaded also on the Pangaea database.

References

Cui, L., Song, X., and Zhong, G.: Comparative Analysis of Three Methods for HYSPLIT Atmospheric Trajectories Clustering, *Atmosphere*, 12, 698, <https://doi.org/10.3390/atmos12060698>, 2021.

Escudero, M., Stein, A., Draxler, R. R., Querol, X., Alastuey, A., Castillo, S., and Avila, A.: Determination of the contribution of northern Africa dust source areas to PM10 concentrations over the central Iberian Peninsula using the Hybrid Single-Particle Lagrangian Integrated Trajectory model (HYSPLIT) model, *J. Geophys. Res.*, 111, D06210, <https://doi.org/10.1029/2005JD006395>, 2006.

Harrison, R. M., Jones, A. M., and Lawrence, R. G.: Major component composition of PM10 and PM2.5 from roadside and urban background sites, *Atmospheric Environment*, 38, 4531–4538, <https://doi.org/10.1016/j.atmosenv.2004.05.022>, 2004.

Karaca, F., Anil, I., and Alagha, O.: Long-range potential source contributions of episodic aerosol events to PM10 profile of a megacity, *Atmospheric Environment*, 43, 5713–5722, <https://doi.org/10.1016/j.atmosenv.2009.08.005>, 2009.

Puxbaum, H., Gomiscek, B., Kalina, M., Bauer, H., Salam, A., Stopper, S., Preining, O., and Hauck, H.: A dual site study of PM2.5 and PM10 aerosol chemistry in the larger region of Vienna, Austria, *Atmospheric Environment*, 38, 3949–3958, <https://doi.org/10.1016/j.atmosenv.2003.12.043>, 2004.

Rolph, G., Stein, A., and Stunder, B.: Real-time Environmental Applications and Display sYstem: READY, *Environmental Modelling & Software*, 95, 210–228, <https://doi.org/10.1016/j.envsoft.2017.06.025>, 2017.

Vardoulakis, S. and Kassomenos, P.: Sources and factors affecting PM10 levels in two European cities: Implications for local air quality management, *Atmospheric Environment*, 42, 3949–3963, <https://doi.org/10.1016/j.atmosenv.2006.12.021>, 2008.